Study of Spatial and Temporal Filtering Techniques and Their Applications in Fiber Optic Communication Systems

By

Hao Wang

Master of Applied Science, School of Electronic Engineering & Optoelectronic Technology, Nanjing University of Science and Technology

A Thesis

Submitted to the School of Graduate Studies

in Partial Fulfillment of the Requirements

for the Degree

Master of Applied Science

McMaster University

by Hao Wang, December, 2007

MASTER OF APPLIED SCIENCE (2007) McMaster University

Electrical and Computer Engineering Hamilton, Ontario

TITLE: Study of Spatial and Temporal Filtering Techniques and Their Applications in Fiber Optic Communication Systems

AUTHOR: Hao Wang, M.A.Sc (Nanjing University of Science and Technology)

SUPERVISORS: Dr. Shiva Kumar and Dr. Changqing Xu

NUMBER OF PAGES: ix, 74

Abstract

This thesis studies spatial and temporal filtering techniques and their applications in fiber optic communication systems. Differential mode delay (DMD) in multimode fibers (MMFs) and multipath interference (MPI) are two major impairments in fiber optic communication systems. DMD lends to inter symbol interference in MMF communication systems which seriously limit the bit rate-distance product of the system. MPI leads to interference pattern at the output of a single mode fiber link which increases the bit error rate of the system. In this thesis, we propose a method which uses spatial filtering technique in a 4F system to reduce DMD and MPI effects. Typically, higher order modes have higher spatial frequency components and therefore, they are spatially separated from the lower mode after Fourier transform. By optimizing the bandwidth of a spatial filter, unwanted higher order modes can be suppressed. Therefore, DMD and MPI effects in fiber optic communication systems can be reduced at the cost of losing some fraction of the signal power.

In this thesis, we also propose a new application of temporal filtering technique. A time lens is a phase modulator which introduces a quadratic phase factor in time domain. Combined with single mode fibers, a time lens can be used to perform Fourier transform in time domain. A tunable optical filter can be implemented using a modified temporal 4F system which is analogy with the spatial 4F system. The merit of this method is that no additional signal processing is needed to reverse the bit sequence at the output of the 4F system and that the channels to be demultiplexed at a node can be dynamically reconfigured.

Acknowledgement

I would like to express my most sincere gratitude to my supervisor, Dr. Shiva Kumar, for his seasoned and patient guidance. He has given me a lot of valuable advices, novel ideas in solving many key problems in my research work. I would also like to thank my co-supervisor Dr. Changqing Xu for his kind assistance and comments. Thanks also go to Dr. Wei-Ping Huang, Dr. Xun Li and Dr. Li Yang who have prepared me in the basic theory of my specialty. The knowledge acquired has allowed me to proceed with this thesis work.

To all other friends and colleagues of the Photonic Research Group at the Department of Electrical and Computer Engineering, I want to express my appreciation for their help and friendship.

Last, but not least, I would like to dedicate this work to my dear wife, Yanping Xi, and parents for their continued love and support.

Contents

List of figures

List of Abbreviations

DFB	Distributed FeedBack
DFE	Decision-Feedback Equalization
DMD	Differential Mode Delay
DRA	Distributed Raman Amplifiers
DRBS	Double Raleigh Back Scattering
EDFA	Erbium Doped Fiber Amplifier
FP	Fabry-Perot
HOF	Hollow Optical Fiber
HOM-DCM	Higher Order Mode Dispersion Compensation Modules
ISI	Intersymbol Interference
LAN	Local Area Network
LE	Linear Equalization
LEAF	Large Effective Area Fiber
LED	Light-Emitting Diode
MLSE	Maximum-Likelihood Sequence Equalization
MMF	Multimode Fiber
MM-DCF	Multimode Dispersion Compensation Fiber
MPI	Multipath Interference
MZ	Mach-Zehnder
NZDSF	Non-Zero Dispersion Shifted Fiber
RMS	Root Mean Square
SMF	Single Mode Fiber
WDM	Wavelength Division Multiplexing
VCSEL	Vertical-Cavity Surface-Emitting Laser

Chapter 1

Introduction

1.1 Introduction to the thesis

Optical fibers have been used in telecommunication areas for many years, both in long haul transmission systems and local area networks (LANs). Optical fibers have such advantages as low cost, low attenuation, no electromagnetic interferences, and large bandwidth, which make it a better choice for wired communications. Optical fibers can be categorized into two major classes, single mode fiber (SMF) and multimode fiber (MMF). Single mode fibers are widely used in long haul transmission systems due to its low attenuation and small dispersion. Multimode fibers are mainly used in some short distance applications, such as LANs and surveillance video. Compared to SMF, MMF has much higher coupling efficiency and is much easier to install.

Depending on the launching conditions, several guided modes can be excited in MMF. Different modes travel in different optical paths and arrive at the end of the fiber at different times, which leads to differential mode delay (DMD). This effect can be detrimental to MMF communication systems since it may lead to serious inter symbol interference (ISI) and limit the bit rate-distance product of the system.

When a standard SMF is used at a wavelength less than cutoff wavelength, it could be bi-modal. In this case, signal travels in fundamental mode (LP_{01} mode) and a weak replica of the signal travels in a higher order mode (LP_{11} mode or LP_{02} mode). Since these two modes have different propagation constants, the interference pattern between these modes

at the output of the fiber leads to multiple path interference (MPI), which can cause performance degradations in fiber optic communication systems.

In this thesis, a spatial filtering method which uses a spatial filter in a 4F system to reduce DMD and MPI effects in MMF and a few mode fibers is proposed. Typically higher order modes are rapidly varying functions along x and y directions, and therefore, they have higher spatial frequency components as compared to the lower order modes. As a result, at the back focal plane of a 4F system, the lower order modes are localized toward the center while the higher order modes are localized towards the edges. Therefore, a properly chosen spatial filter could filter out a large fraction of unwanted modes which lead to DMD or MPI at the cost of losing a fraction of signal power. Our simulation results shows that using spatial filters in a 4F system, the DMD in MMFs can be reduced. Under restricted launching condition with no offset, rms pulse width can be reduced up to 58.9% with only 0.99 dB power loss of the signal using a low pass spatial filter. Our simulation results also shows that as the MPI reduction factor increases, the signal power loss also increases and thus, there is a trade off between the two. By optimizing the spatial filter bandwidth, MPI reduction factor can be as large as 6 dB, while the power loss of LP_{01} mode is 1.7 dB.

A new application of temporal filtering using a temporal 4F system consisting of time lens and single mode fibers to implement a tunable optical filter is also proposed in this thesis. A time lens is actually a phase modulator which introduces a quadratic phase factor in time domain. Combined with some dispersive mediums, such as single mode fibers, a time lens can be used to perform Fourier transform in time domain. This is an exactly analogy with the spatial 4F system. Using this method, the channels to be

demultiplexed at a node in wavelength division multiplexing systems (WDMs) can be dynamically reconfigured. The concept is verified by simulation results.

1.2 Introduction to chapters

The thesis is organized as follows:

In chapter 1, a brief introduction about the work of this thesis is given and the content of each chapter. The main contribution of this thesis is also summarized in this chapter.

In chapter 2, the basic concept of MMFs, DMD and MPI are introduced. Previous researches that have been done related to DMD and MPI reductions in MMFs are reviewed.

In chapter 3, the basic concept of spatial and temporal filtering is reviewed. The applications of spatial and temporal 4F system using lenses are stated.

In chapter 4, the mathematical analyses of DMD in MMFs under restricted launching conditions and MPI in a few mode fibers are given. The application of using spatial filtering to reduce DMD and MPI are proposed and demonstrated using simulation results.

In chapter 5, the application of using temporal filtering to implement tunable optical filter is proposed and demonstrated using simulation results. .

In chapter 6, the work in the thesis is concluded.

1.3 Contribution

The main contributions of this thesis are as follows:

1. We proposed a method to reduce DMD effect in MMF and MPI effect in a few mode fibers using a spatial filter in 4F system. Simulation result shows that under restricted launching condition with no offset, rms pulse width can be reduced up to 58.9% with only 0.99 dB power loss of the signal using a low pass spatial filter. Our simulation results also shows that by optimizing the spatial filter bandwidth, MPI reduction factor can be as large as 6 dB, while the power loss of LP01 mode is 1.7 dB.

2. We proposed a method that uses temporal filtering in a temporal 4F system consisting of time lens and single mode fibers to implement tunable optical filter. The advantage of the proposed scheme is that the channels to be demultiplexed at a node can be dynamically reconfigured.

The research work has resulted in the following publications

1. H. Wang, S. Kumar and C. Xu, "Reduction of multipath interference in a few mode fibers using spatial filters", proceedings of SPIE, Volume 6695, 2007.

2. H. Wang, S. Kumar and C. Xu, "Multiple Path Interference and Differential Modal Delay Reduction Using Spatial Filters in a 4F System", submitted to Journal of Applied Optics, OSA, 2007.

3. D. Yang, S. Kumar and H. Wang, "Temporal filtering using time lenses for optical transmission systems", Journal of Optics Communications, 2007, accepted for publication.

Chapter 2

Research Background: Differential Mode Delay and Multipath Interference in Multimode Fibers

2.1 Introduction to multimode fiber

Multimode fiber (MMF) has been widely used in short distance applications, such as on campus or within buildings for many years because of its high capacity and reliability. MMF can support applications from 10 Mbps to 10 Gbps over length of up to several hundred meters. The coupling efficiency from the light source to MMF is higher than that of the mode fiber (SMF) due to its larger core diameter. Usually, MMFs are described by their core and cladding diameters. So 50/125 μm MMF has a core diameter of 50 μm and a cladding diameter of 125 μm. The most widely deployed MMFs in practical situations are 50/125 μm and 62.5/125 μm.

MMFs are usually classified into two types according to their core refractive index profiles. As shown in Fig. 2.1, if the refractive index in the core is uniform, the MMF is called step index MMF. If the refractive index profile in the core changes gradually, the MMF is called graded index MMF. In Fig. 2.1, $n(r)$ is refractive index profile, n_1 is refractive index of the core center, n_2 is refractive index of the cladding and Δ is relative refractive index difference and is given by

$$\Delta = \frac{n_1^2 - n_2^2}{2n_1^2} \tag{2.1}$$

These two MMFs have different properties due to their different core refractive index profiles. They find their applications in different situations in fiber optic communication systems.

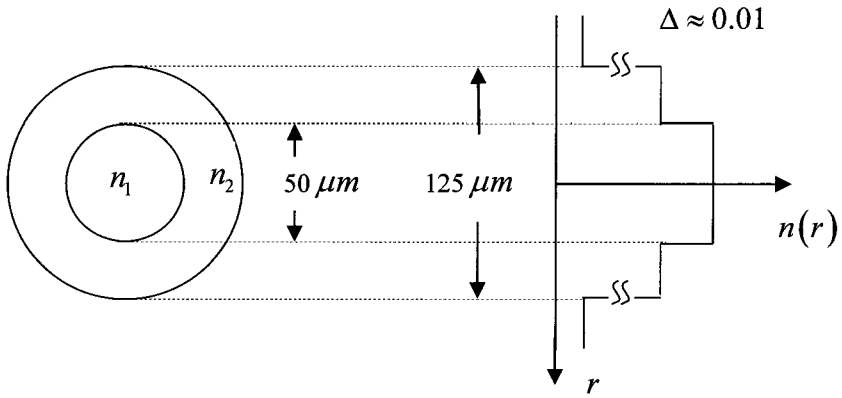

(a) Step index MMF

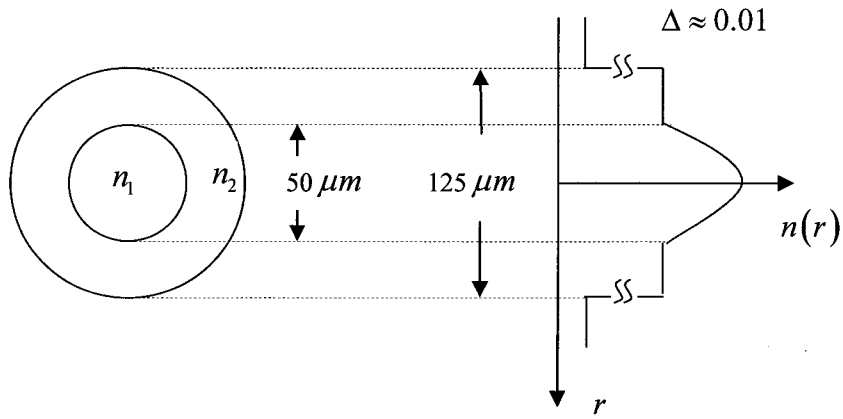

(b) Graded index MMF

Figure2.1: Typical dimensions and refractive index profiles of MMFs

2.2 Differential mode delay in multimode fibers

In MMFs, light can travel in different optical paths, which are called modes. The number of modes that a MMF can support depends on the core radius, the relative refractive

index difference of the MMF and the wavelength of the input light. Different modes have different group velocities and travel in different optical paths, which make them arrive at the output end of the fiber link at different times. So a narrow optical pulse at the input end will be broadened after transmitting some distance in a MMF. This effect is called differential mode delay (DMD). It can be detrimental to MMF communication systems since it may lead to serious inter symbol interference (ISI). The bit rate-distance product of the system is greatly limited by this effect.

The refractive index profile of a MMF has a strong effect on DMD. The graded index MMF has much smaller DMD than the step index MMF [1]. This is because in a graded index MMF, the mode that travels the longest path has the largest group velocity and the mode that travels the shortest path has the smallest group velocity, so the time difference of arrival between different modes at the end of the fiber has been reduced greatly.

DMD in a MMF also depends strongly on the launching conditions. In the case of overfilled launch, such as using LED in the transmitter, all modes supported by the MMF are equally excited; this leads to serious DMD effect. In the case of restricted launch, such as using vertical-cavity surface-emitting laser (VCSEL) or distributed feedback (DFB) lasers in the transmitter, different launching positions excite different mode combinations, which lend to different DMD effect[2][3]. In most cases, restricted launch has a smaller DMD than overfilled launch.

Under overfilled launch, all modes are excited with equal power. DMD is measured by the difference of arrival time between the fastest mode and the slowest mode. In the step index MMF, according to ray optics, the maximum time delay is given by [4]:

$$\Delta T = \frac{Ln_1}{c}\left(\frac{n_1}{n_2} - 1\right) \approx \frac{n_1 \Delta L}{c} \tag{2.2}$$

where L is transmission length, n_1 is the refractive index of the core, n_2 is the refractive index of the cladding, Δ is relative refractive index difference, c is the velocity of light in vacuum.

In the graded index MMF, the refractive index profile is given by the following formula:

$$n(r) = \begin{cases} n_1\left[1 - 2\Delta\left(\frac{r}{a}\right)^{\alpha}\right]^{\frac{1}{2}} & r < a \quad (core) \\ n_1\left(1 - 2\Delta\right)^{\frac{1}{2}} = n_2 & r \geq a \quad (cladding) \end{cases} \tag{2.3}$$

where r is the radial distance from the core center. α is the profile parameter. When $\alpha = 2$, the refractive index profile is parabolic. When $\alpha = 2(1-\Delta)$, the maximum time delay is minimized and is given by [4]

$$\Delta T \approx \frac{n_1 L \Delta^2}{8c} \tag{2.4}$$

$\alpha = 2(1-\Delta)$ is the optimum profile parameter for a graded index MMF for the reduction of DMD. Eqs. (2.3), (2.5) show that, under the same launching condition, the graded index MMF has much smaller DMD than the step index MMF. Therefore, using graded

index MMF with optimum index profile instead of step index MMF can greatly reduce DMD effect.

A significant research has been done to reduce DMD effect in MMF communication systems, such as using multimode dispersion compensation fibers (MM-DCF) [5], different launching schemes [6-7] and using equalization techniques [8-10].

1. MM-DCF

   The basic concept of MM-DCF scheme is to realize the optimum refractive index profile by concatenating the target fiber with a MM-DCF. The refractive index profile of MM-DCF is specially designed to compensate the discrepancy of the refractive index profile of the target fiber from the optimum refractive index profile. So the target fiber combined with a MM-DCF provides an optimum refractive index profile which reduces DMD.

2. Different launching schemes

   As mentioned above, using laser instead of LED in the transmitter leads to much smaller DMD effect. It is also found that different launching schemes using laser may cause different DMD effects. Using a laser diode or a single mode fiber to launch light into the center of the MMF, only a small number of lower order modes are excited, which leads to small DMD effect. The mode converter based on hollow optical fiber (HOF) transforms the fundamental mode of a single mode fiber to a ring shaped mode. Using this mode converter to launch light into the

MMF, only a few higher order modes can be excited selectively, which also leads to small DMD effect.

3. Equalization

Equalization is a technique used in communication systems to mitigate ISI effect. There are basically three types of equalization methods: linear equalization (LE), decision-feedback equalization (DFE), and maximum-likelihood sequence equalization (MLSE). In MMF communication systems, equalization can be done both in electrical domain and in optical domain to reduce DMD effect.

Electrical domain equalization can be implemented after the photo detector using nonlinear DFE [8]. The basic principle can be described as follows. Supposing only three modes were excited in the MMF, the modal delays between them are t_1 and t_2 after propagating some distance in the fiber. If the equalizer is working, it can regenerate the input signal pulse at the output of the decision circuit. The signal pulse is feedback to the input of the decision circuit with delays (t_1 and t_2, respectively) and mode weighting factors. After subtracting them from the input, the multipath components are cancelled. A pulse without DMD effect can be obtained. Adaptive algorithms can also be included in the system to implement adaptive equalization.

Optical equalization can be implemented using multi-segmented photo detector [9-10]. Assuming a two segmented photo detector is used in the system, the two

photo detector segments detect different combination of multiple modes in the MMF. By subtracting these two sub-signals and then spatially isolating the lower order modes from higher order modes, DMD effects can be reduced easily.

2.3 Multipath interference in a few mode fibers

In fiber optic communication systems, multiple path interference (MPI) is one of the major impairments that can degrade system performance. MPI is caused by the beating between a signal and its weak replica. In systems using distributed Raman amplifiers (DRA), MPI is caused by the interference between a signal and a weak replica resulting from double Raleigh back scattering effect (DRBS) [11]. In wavelength division multiplexing (WDM) systems, the add-drop nodes in the multiplexers and demultiplexers pairs can also lead to MPI [12] due to imperfect filter isolation in the nodes. MPI can also be found in fiber transmission systems with multiple connectors due to discrete reflections [13].

MPI also occurs in fibers that support multiple modes. For example, in the standard single mode fiber (SMF) fiber, if the laser wavelength is less than the cutoff wavelength of the fiber, the fiber can support two modes (LP_{01} and LP_{11}). Even if the LP_{01} mode is launched at the fiber input, a fraction of the power is transferred to LP_{11} mode due to refractive index imperfections and thus, a replica of the signal propagates as LP_{11} mode. Since the optical path length of the higher order mode is different from the fundamental mode, it leads to interference pattern at the output end of the fiber. Non-zero dispersion

shifted fiber (NZDSF) such as large effective area fiber (LEAF) [14] could become bi-modal when the wavelength $\lambda \leq 1.3\mu m$. This is because some of the desirable attributes such as large effective area, relatively low dispersion and low dispersion slope can be obtained only if the cut-off wavelength is higher [14]. In such a fiber, most of the signal power propagates as LP_{01} mode. But refractive index fluctuations due to micro-bending could cause the power coupling to LP_{11} mode. Since these two modes have different propagation constants, the interference between these modes can cause performance degradations in fiber optic communication systems. Some of the fibers used in erbium doped fiber amplifiers (EDFA) become bi-modal at the pump wavelength $\lambda = 980nm$ resulting in MPI and performance degradations. This multiple modes-induced MPI can also be found in higher order mode dispersion compensation modules (HOM-DCM) which is used in long haul fiber optic transmission systems [15]. In HOM-DCM, the signal propagates as LP_{02} mode. At the end of the HOM-DCM, a mode converter is placed to convert LP_{02} mode to LP_{01} mode and MPI is caused by the interference between LP_{01} mode and LP_{02} mode at the output end of the fiber link. This kind of MPI can be reduced by using specifically designed optical waveguide that suppresses the unwanted modes [16].

2.4 Conclusion

In this chapter, the basic concepts of MMFs were introduced. The origins of two major impairments, DMD and MPI, in fiber optic communication systems were explained in details. Research related to reduce DMD and MPI effects were reviewed.

Chapter 3

Research Background: Spatial and Temporal Filtering

3.1 Introduction

Lenses are very important components in optical imaging and data processing systems. A very important property of a thin lens is its Fourier transforming property. Working with a suitable spatial filter, a thin lens could be used to perform spatial frequency filtering, which modifies some attributes of a spatial filed distribution. A thin lens introduces a quadratic phase factor, $\exp\left(j\alpha x^2\right)$ and therefore, it converts a plane wave front to a spherical wave front. The time analogue of space lens is a "time lens" which introduces a quadratic phase factor, $\exp\left(j\alpha t^2\right)$.The time lens can be realized using a phase modulator. Combined with a dispersive medium, such as a single mode fiber, time lens can be used to perform Fourier transform in time domain. This property can be used in many applications in fiber optic communication systems. In this chapter, The Fourier transforming property of a spatial lens and a time lens are introduced. Their applications in spatial and temporal filtering are analyzed.

3.2 The Fourier transforming property of a thin lens

Lenses are simple optical devices which transmit and refract light. A lens is said to be a thin lens if the thickness between two faces of the lens is negligible compared to the focal length of the lens. According to [17], the lens can be represented as a phase transforming function

$$P(x,y)=\exp\left(jkd_m\right)\exp\left[jk(n-1)d(x,y)\right] \tag{3.1}$$

where k is the wave number of the light in vacuum, n is the refractive index of the lens, d_m is the maximum thickness of the lens and $d(x,y)$ is the thickness at coordinates (x,y) (see Fig. 3.1). Using the paraxial approximation [17], Eq. (3.1) can be simplified as

$$P(x,y) = \exp\left[-j\frac{k}{2f}\left(x^2+y^2\right)\right] \tag{3.2}$$

where f is the focal length of the lens, which is defined by

$$\frac{1}{f} = (n-1)\left(\frac{1}{R_1} - \frac{1}{R_2}\right) \tag{3.3}$$

where R_1 and R_2 are radii of curvature of the left surface and right surface of the lens, respectively.

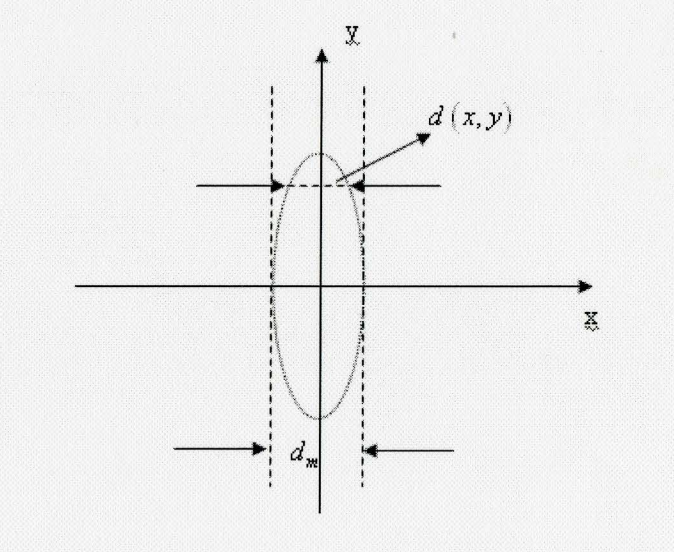

Figure3.1: The side view of a thin lens

Assuming the field distribution of the light at the left surface of the lens is $U_l(x,y)$, the field distribution of the light at the right surface of the lens is given by

$$U_r = U_l(x,y)P(x,y) \tag{3.4}$$

If the incident field distribution of the light at a distance z in front of the lens is $U_i(x,y)$, according to Fresnel diffraction [1], the field distribution at a distance f behind the lens (back focal plane of the lens) is given by

$$U_f(u,v) = \frac{\exp\left[j\frac{k}{2f}\left(1-\frac{z}{f}\right)\left(u^2+v^2\right)\right]}{j\lambda f}\int_{-\infty}^{\infty}\int_{-\infty}^{\infty}U_i(x,y)\exp\left[-j\frac{2\pi}{\lambda f}(xu+yv)\right]dxdy \tag{3.5}$$

When $z = f$, i.e. the incident field distribution is in the front focal plane of the lens, Eq. (3.5) becomes

$$U_f(u,v) = \frac{1}{j\lambda f}\int_{-\infty}^{\infty}\int_{-\infty}^{\infty}U_i(x,y)\exp\left[-j\frac{2\pi}{\lambda f}(xu+yv)\right]dxdy \tag{3.6}$$

This is an exactly two dimensional Fourier transform except for the unimportant constant $\frac{1}{j\lambda f}$. Therefore, if the input field distribution is in the front focal plane of a lens, the Fourier transform of the field distribution can be obtained in the back focal plane of the lens. This is the Fourier transforming property of a thin lens. $\left(\frac{u}{\lambda f},\frac{v}{\lambda f}\right)$ are usually referred to as the spatial frequencies.

3.3 Spatial filtering using thin lens

From Eq. (3.6) we have seen that, if the incident field distribution locates in the front focal plane of a lens, the spatial frequency distribution of the incident field can be obtained at the back focal plane of the lens. This is called a 2F system. The lower spatial frequency components are located in the center of the back focal plane while the higher spatial frequency components are located at the edges. The spatial frequency components of the field can be modified by putting a suitable spatial filter (low pass, high pass, band pass or band stop) in the back focal plane of the lens. This is the basis of spatial frequency filtering.

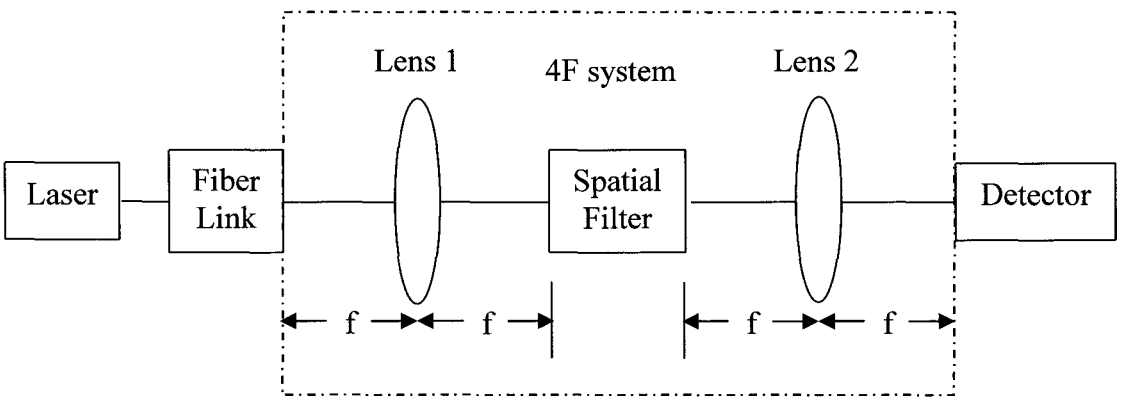

Figure3.2: The setup of a 4F system

Two 2F systems can be cascaded together (as shown in Fig. 3.2) to form a 4F system. In the absence of the spatial filter, this 4F system leads to the Fourier transform of the Fourier transform of the incident field distribution which is nothing but an inverted image

of the incident field distribution. This 4F system is widely used for optical signal processing applications, such as image processing, nonlinear optical measurement [18] and joint transform correlator [19].

3.4 Temporal filtering using time lenses

3.4.1 The analogy between spatial diffraction and temporal dispersion

Assuming the incident field distribution in spatial domain at $z=0$ is $U_i(x,y,z=0)$, it can be represented by its Fourier transform as

$$U_i(x,y,z=0)=\int_{-\infty}^{\infty}U_f(u,v,z=0)\exp\left[j2\pi(xu+yv)\right]dudv \tag{3.7}$$

where $U_f(u,v,z=0)$ is the Fourier transform of $U_i(x,y,z=0)$, (u,v) are spatial frequencies. According to Fresnel diffraction [17], at a distance z, the field distribution in spatial frequency domain can be written as

$$U_f(u,v,z)=U_f(u,v,z=0)\exp\left[-j\pi\lambda z\left(u^2+v^2\right)\right] \tag{3.8}$$

So the field distribution in spatial domain can be written as

$$U_z(x,y,z)=\int_{-\infty}^{\infty}U_f(u,v,z=0)\exp\left[-j\pi\lambda z\left(u^2+v^2\right)\right]\exp\left[j2\pi(xu+yv)\right]dudv \tag{3.9}$$

where the term $\exp\left[-j\pi\lambda z\left(u^2+v^2\right)\right]$ is known as spatial dispersion term.

Next, let us consider the signal propagation in a single mode optical fiber. Suppose the electric field envelope at $z=0$ is $g(t,z=0)$. It can be represented using its Fourier transform as

$$g(t,z=0)=\int_{-\infty}^{\infty}G(f)\exp(j2\pi ft)df \tag{3.10}$$

After propagating a distance z in a SMF, the signal in a reference frame that is attached to the signal can be as

$$g(t,z)=\int_{-\infty}^{\infty}G(f)\exp\left(-j\beta^{''}zf^2\right)\exp(j2\pi ft)df \tag{3.11}$$

where $\beta^{''}$ is the dispersion coefficient of the single mode optical fiber. Comparing Eq. (3.9) and Eq. (3.11), we can see that there exists exactly analogy between spatial diffraction and temporal dispersion.

3.4.2 The analogy between time lens and spatial lens

As discussed in Section 3.2, a spatial thin lens introduces a quadratic phase factor and its phase transforming function can be written as

$$P(x,y)=\exp\left(-j\frac{k}{2f}\left(x^2+y^2\right)\right) \tag{3.12}$$

The time lens can be implemented using a phase modulator whose time domain transfer function is given by

$$L(t) = \exp[j\xi V(t)] \tag{3.13}$$

where $V(t)$ is the applied voltage to the phase modulator, ξ is the phase modulation index and t is the time variable in a reference frame that moves with the optical pulse. To achieve the quadratic phase modulation, the voltage can be chosen as

$$V(t) = \alpha t^2 \tag{3.14}$$

Using Eq. (3.13) in Eq. (3.14), the function of the time lens becomes

$$L(t) = \exp[j\xi\alpha t^2] \tag{3.15}$$

Comparing Eq. (3.12) and Eq. (3.15), we can see the analogy between the spatial lens and the time lens. According to [20], the focal length of the time lens is be given as

$$F = 1/(2|\beta''\xi\alpha|) \tag{3.16}$$

The Fourier transform of the transfer function (Eq.3.15) can be written as

$$L_f(\omega) = \sqrt{j\pi/\xi\alpha}\exp\left(-j\frac{\omega^2}{4\xi\alpha}\right) \tag{3.17}$$

3.4.3 Temporal filtering using 4F systems with time lenses

As discussed in section 3.3, a 2F system with a spatial lens can perform Fourier transform of the incident spatial field distribution. A spatial filter can be utilized at the back focal plane of the lens to modify the spatial frequency components of the incident field.

Another 2F system cascaded to the first one can transform the modified field back to spatial domain. This whole system is called a 4F system in spatial domain. Similarly, a temporal 4F system can be implemented using SMFs and time lenses as shown in Fig. 3.4.

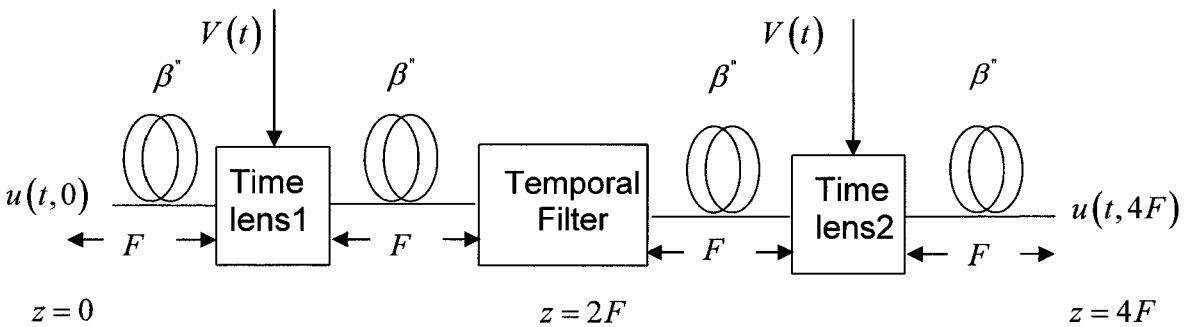

Figure3.3: Temporal 4F system using SMFs and time lens

Assuming the input signal of this temporal 4F system is $u(t,0)$, it can be represented as

$$u(t,0)=\frac{1}{2\pi}\int_{-\infty}^{\infty}\tilde{u}(\omega,0)\exp(-j\omega t)d\omega \tag{3.18}$$

where $\tilde{u}(\omega,0)$ is the Fourier transform of $u(t,0)$. The signal immediately before the time lens, the is given by

$$u(t,F_{-})=\frac{1}{2\pi}\int_{-\infty}^{\infty}\tilde{u}(\omega,0)\exp\left(\frac{j\beta^{"}F\omega^{2}}{2}\right)\exp(-j\omega t)d\omega \tag{3.19}$$

The function of the time lens is a to multiply the input signal by a quadratic phase factor in time domain, the signal immediately after the time lens is given by

$$\begin{aligned} u(t,F_+) &= u(t,F_-)\times L(t) \\ &= \frac{1}{2\pi}\int_{-\infty}^{\infty} \%(\omega-\Omega,F_-)L_f(\Omega)d\Omega \end{aligned} \tag{3.20}$$

At the back focal plane of the first time lens, the signal is given by

$$u(t,2F) = \frac{1}{2\pi}\int_{-\infty}^{\infty} \%(\omega,F_+)\exp\left(\frac{j\beta'' F\omega^2}{2}\right)\exp(-j\omega t)d\omega \tag{3.21}$$

Using Eq. (3.15-3.21), the above equation can be solved as

$$u(t,2F) = \frac{\sqrt{j\pi/\xi\alpha}}{2\pi|\beta'' F|}\%\left(\frac{t}{\beta'' F},0\right) \tag{3.22}$$

So at the back focal plane of the first time lens, the temporal signal is proportional to the Fourier transform of the signal at the front focal plane of the first lens. Using a temporal filter at the back focal plane of the first lens, the attributes of the signal can be modified in time domain. If there is no temporal filter at the back focal plane of the first lens, following the same approach as above, the signal at the output of the 4F system can be written as

$$u(t,4F) = u(-t,0) \tag{3.23}$$

In deriving Eq. (3.23), an unimportant constant factor is ignored. From Eq. (3.23), we know that without the temporal filter, the 4F system leads to the Fourier transform of the Fourier transform of the input signal. The output signal is exactly the same as the input signal except that it is reversed in time.

This 4F system can be used in many applications in fiber optic communication systems, such as simple imaging, correlation, convolution, and joint transform processor [21]. Using different configurations, it can also be used to implement tunable optical filter in WDM system and higher-order dispersion compensator [22]. Using a temporal filter at the back focal plane of the first time lens, the signal from the desired channel can be filtered out at the output of the 4F system. But the bit sequence is reversed in time. Additional signal processing functions in optical or electrical domains are needed to recover the original bit sequence.

3.5 Conclusion

In this chapter, the Fourier transforming property of a spatial lens and a time lens were analyzed. The concepts of spatial and temporal filtering were introduced. Their potential applications in fiber optic communication systems were stated.

Chapter 4

Reduction of DMD and MPI Using Spatial Filtering

4.1 Introduction

DMD and MPI are two major impairments in fiber optic communication systems. Depending on the launching conditions, several guided modes can be excited in MMFs. Different modes travel in different optical paths and arrive at the end of the fiber at different times, which leads to DMD. This effect can be detrimental to MMF communication systems since it may lead to serious inter symbol interference (ISI) and limit the bit rate-distance product of the system. DMD can be reduced using graded index MMF with optimum index profile, multimode dispersion compensation fibers [5], different launching schemes to selectively excite lower order modes [6] or higher order modes [7], or by using equalization techniques [8-10].

As discussed in chapter 2, MPI effect can be found in bi-modal fibers. The standard SMFs become bi-modal if the laser wavelength is less than the cutoff wavelength. In this case, the fiber can support two modes (LP_{01} and LP_{11}). Even if the LP_{01} mode is launched at the fiber input, a fraction of the power is transferred to LP_{11} mode due to refractive index imperfections and thus, a replica of the signal propagates as LP_{11} mode. Since the optical path length of the higher order mode is different from the fundamental mode, it leads to interference pattern at the output end of the fiber. Similar phenomenon can also be found in systems that use Non-zero dispersion shifted fiber (NZDSF) such as large effective area fiber (LEAF). This multiple modes-induced MPI can also be found in higher order mode dispersion compensation modules (HOM-DCM). In HOM-DCM, the signal propagates as LP_{02} mode. At the end of the HOM-DCM, a mode converter is

placed to convert LP_{02} mode to LP_{01} mode and MPI is caused by the interference between LP_{01} mode and LP_{02} mode. As reviewed in chapter 2, this kind of MPI can be reduced by using specifically designed optical waveguide that suppresses the unwanted mode [16].

In this chapter, a new method is proposed to reduce DMD and MPI effects in fiber optic communication systems using spatial filtering concept. The mathematical analysis of DMD in a MMF under restricted launch conditions and MPI in a few mode fibers are carried out. The impact of launching offset on DMD is simulated. Simulation results show that both effects can be reduced effectively at the cost of losing some signal power.

4.2 DMD reduction using spatial filters

4.2.1 Mathematical analysis of DMD in MMFs under restricted launching conditions

In order to increase the capacity of the MMF communication system, laser is used at the transmitter instead of LED. Unlike under overfilled launching conditions, modes are selectively excited with unequal power distributions under restricted launching conditions. Eq. (2.3) and Eq. (2.5) can not be used to calculate DMD under these launching conditions. In this thesis a new method is developed according to wave optics to measure the DMD effect under such launching conditions.

At the input end of the fiber, optical field distribution can be written as

$$\Psi(x,y,z=0,t)=\phi(x,y)f(t) \tag{4.1}$$

where $\phi(x,y)$ is the spatial distribution of the pulse at $z=0$, and $f(t)$ is the temporal pulse. It is known that the modes of an optical fiber form a complete orthogonal basis, so an arbitrary spatial field distribution can be expanded in terms of these modes as [1].

$$\phi(x,y)=\sum_{n=1}^{N} a_n\varphi_n(x,y) \tag{4.2}$$

where $\varphi_n(x,y)$ is the nth guided mode distribution, and a_n is the weight factor of the nth mode. In Eq. (4.2), we ignore the radiation modes since they are strongly attenuated. Multiplying Eq. (4.2) by $\varphi_n(x,y)$ at $z=0$ and integrating over the cross section of the fiber, we obtain

$$a_n=\iint\phi(x,y)\varphi_n(x,y)dxdy \tag{4.3}$$

Eq. (4.1) can be rewritten as

$$\Psi(x,y,z=0,t)=\frac{\phi(x,y)}{2\pi}\int_{-\infty}^{\infty}F(\omega)\exp(-j\omega t)d\omega \tag{4.4}$$

where $F(\omega)$ is the Fourier transform of $f(t)$. Using Eq. (4.2) in Eq. (4.4), we obtain

$$\Psi(x,y,z=0,t)=\frac{1}{2\pi}\sum_{n=1}^{N}\int_{-\infty}^{\infty}a_n\varphi_n(x,y)F(\omega)\exp(-j\omega t)d\omega \tag{4.5}$$

Since each frequency component propagates independently, the field at an arbitrary distance z is given by

$$\Psi(x,y,z,t)=\frac{1}{2\pi}\sum_{n=1}^{N}\int_{-\infty}^{\infty}a_n\varphi_n(x,y)F(\omega)\exp\left\{-j\left[\omega t-\beta_n(\omega)z\right]\right\}d\omega \tag{4.6}$$

where $\beta_n(\omega)$ is the propagation constant of the n^{th} mode. Typically the signal bandwidth is much smaller than the carrier frequency and therefore the function $F(\omega)$ is sharply peaked around the carrier frequency ω_c and in this narrow frequency domain, we assume a_n and $\varphi_n(x,y)$ to be independent of frequency. Making the Taylor series expansion of β_n around $\omega=\omega_c$

$$\beta_n(\omega)=\beta_{n0}+\beta_n^{'}(\omega-\omega_c)+\beta_n^{''}(\omega-\omega_c)^2/2+\cdots \tag{4.7}$$

where $\beta_{n0}=\beta_n(\omega_c)$, $\beta_n^{'}=\left.\frac{d\beta_n}{d\omega}\right|_{\omega=\omega_c}$, and $\beta_n^{''}=\left.\frac{d^2\beta_n}{d\omega^2}\right|_{\omega=\omega_c}$. $\beta_n^{'}$ is the inverse group velocity of the n^{th} mode and $\beta_n^{''}$ is the dispersion coefficient of the n^{th} mode. If the signal bandwidth is much smaller than the carrier frequency ω_c, we can truncate the Taylor series after the third term without losing much accuracy. To make the expression simpler, we choose the variable Ω as

$$\Omega=\omega-\omega_c \tag{4.8}$$

Using Eq. (4.7) and Eq. (4.8), Eq. (4.6) becomes

$$\begin{aligned}\Psi(x,y,z,t)=&\frac{1}{2\pi}\sum_{n=1}^{N}a_n\varphi_n(x,y)\exp\left[-j\left(\omega_c t-\beta_{n0}z\right)\right]\\&\times\int_{-\infty}^{\infty}F(\Omega)\exp\left[j\left(\beta_n^{'}\Omega z+\beta_n^{''}\Omega^2 z/2\right)\right]\exp(-j\Omega t)d\Omega\end{aligned} \tag{4.9}$$

Let us define

$$H_n(\Omega) = \exp\left[j\left(\beta_n'\Omega z + \beta_n''\Omega^2 z/2\right)\right] \tag{4.10}$$

where $H_n(\Omega)$ is called fiber transfer function corresponding to the nth mode. Using Eq. (4.10) in Eq. (4.9), we obtain

$$\Psi(x,y,z,t) = \frac{1}{2\pi}\sum_{n=1}^{N} a_n\varphi_n(x,y)\exp\left[-j\left(\omega_c t - \beta_{n0}z\right)\right]\int_{-\infty}^{\infty} F(\Omega)H_n(\Omega)\exp(-j\Omega t)\,d\Omega \tag{4.11}$$

For multimode fiber communication systems, the intermodal dispersion is dominant and therefore, the effect of the intramodal dispersion can be ignored, i.e. $\beta_n'' \cong 0$. Now the field distribution at an arbitrary distance z is given by

$$\Psi(x,y,z,t) = \frac{1}{2\pi}\sum_{n=1}^{N} a_n\varphi_n(x,y)\exp\left[-j\left(\omega_c t - \beta_{n0}z\right)\right] f\left(t-\beta_n' z\right) \tag{4.12}$$

where

$$f\left(t-\beta_n' z\right) = \int_{-\infty}^{\infty} F(\Omega)H_n(\Omega)\exp(-j\Omega t)\,d\Omega \tag{4.13}$$

The optical power is given by

$$P(t,z) = \iint \left|\Psi(x,y,z,t)\right|^2 dxdy \tag{4.14}$$

Using the orthogonal relation

$$\iint \varphi_m(x,y)\varphi_n^*(x,y)\,dxdy = \delta_{mn} \tag{4.15}$$

where δ_{mn} is Kronecker delta function, Eq. (4.14) becomes

$$P(t,z)=\frac{1}{(2\pi)^2}\sum_{n=1}^{N}a_n^2 f^2\left(t-\beta_n' z\right) \tag{4.16}$$

The photodetector current is proportional to the optical power and given by

$$I(t)=RP(t,z), \tag{4.17}$$

where R is responsivity of the photodetector. In order to determine the DMD caused by intermodal dispersion, the pulse spread should be measured at the receiver. The rms pulse width is often used to measure the pulse spread [23], and is defined as

$$\sigma_{rms}=\left(\frac{\int_{-\infty}^{\infty}t^2\left|I(t)\right|^2dt-\left(\int_{-\infty}^{\infty}t\left|I(t)\right|^2dt\right)^2}{\int_{-\infty}^{\infty}\left|I(t)\right|^2dt}\right)^{\frac{1}{2}}. \tag{4.18}$$

The pulse broadening due to DMD in MMFs can be measured by calculating σ_{rms} at the receiver.

The above analysis based on the assumption that the cross section of the MMF is smaller than the cross section of the photo detector. In this case, all optical power can be coupled into the photo detector. Using modes orthogonal property, there are no cross terms after the integral of the power density over the cross section, which means there is no multipath interference (MPI) effect(refer to section.4.3). If the cross section of the MMF is larger than the cross section of the photo detector, only a fraction of the signal power is coupled into the photo detector. In this case, cross terms could leads to MPI effect.

4.2.2 The impact of launching offset on DMD under restricted launching conditions

Before simulating DMD effect in MMFs, a mode solver is necessary for calculating mode distributions in the fiber. In order to verify the mode solver, the inter-modal dispersion is calculated using the following formula

$$D = \beta_{\max}^{'} - \beta_{\min}^{'} \tag{4.19}$$

where $\beta_{\max}^{'}$ is the maximum value of inverse group velocity of modes in the MMF and $\beta_{\min}^{'}$ is the minimum value of inverse group velocity of modes in the MMF. Both $\beta_{\max}^{'}$ and $\beta_{\min}^{'}$ are obtained by using mode solver.

Using the following parameters in the mode solver, the refractive index at the core center, 1.5, relative refractive index difference, 0.01, and the wavelength of the incident light, 0.85 μm, the variation of inter-modal dispersion with fiber refractive index profile parameter α can be obtained, as shown in Fig. 4.1, which is matched with the results in [24].

As discussed in section 2.1 and also shown in Fig. 4.1, when $\Delta = 0.01$, $\alpha = 1.98$ is the optimized profile parameter in the sense of DMD under overfilled launch. In the following simulation, we investigate the impact of profile parameter of the graded index MMF on DMD under restricted launch. The parameters used in the simulation are as follows: the wavelength of the incident light, $1.3\mu m$, core diameter of the fiber, $62.5\mu m$,

refractive index at core center, 1.491, relative refractive index difference, 0.01, laser spot size (FWHM)= 7 μm, and temporal pulse width (FWHM)=50 ps.

The RMS pulse width at the output of a MMF in Fig.4.2 is calculated using Eq.(4.18). The results show that when $\Delta = 0.01$, $\alpha = 1.98$ leads to minimum DMD effect under both overfilled launching condition and restricted launching condition. The results also show that restricted launch with no offset results in a much smaller DMD than overfilled launch.

Under restricted launch, different launching offsets excite different mode combinations with different mode power distributions, which lead to different DMD effects at the output end of the fiber. Next, we investigate the impact of launching offset on DMD under restricted launch. The parameters in the simulation are the same as the simulation above.

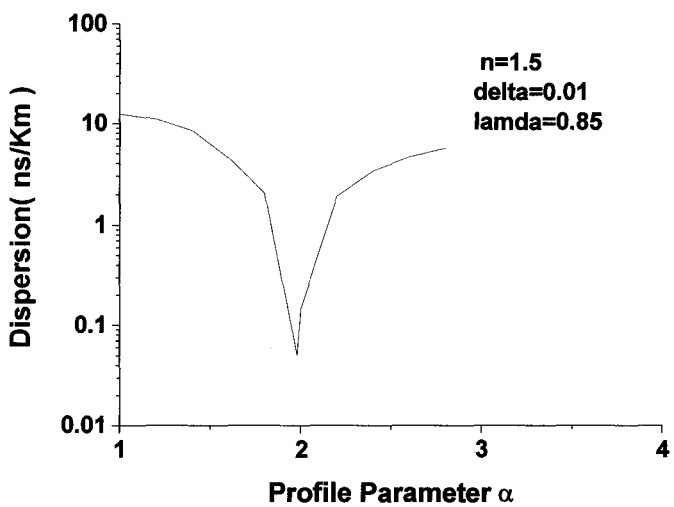

Figure4.1: Variation of inter-modal dispersion with the profile parameter α for a graded index MMF

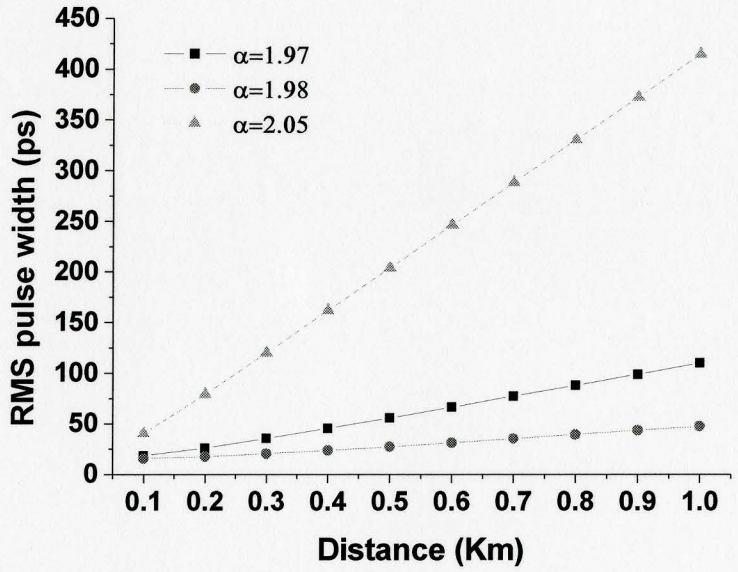

(a)

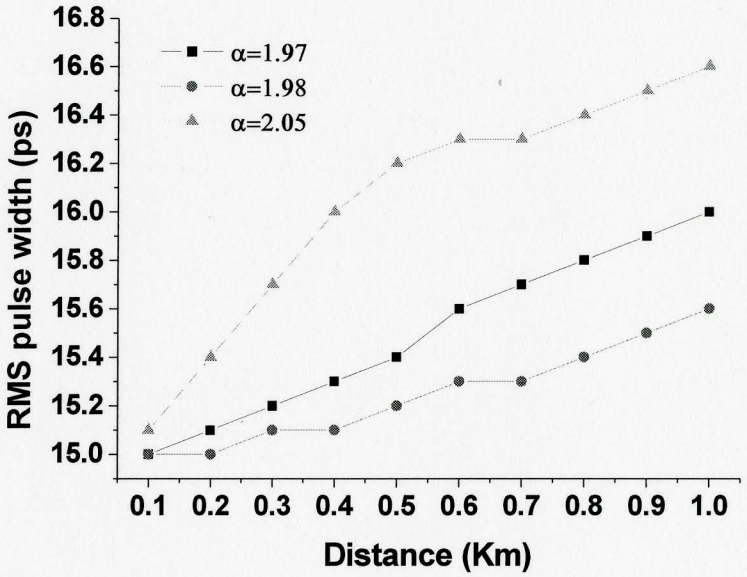

(b)

Figure4.2: RMS pulse width as a function of propagation distance at different profile parameters. (a) overfilled launch; (b) restricted launch with no offset.

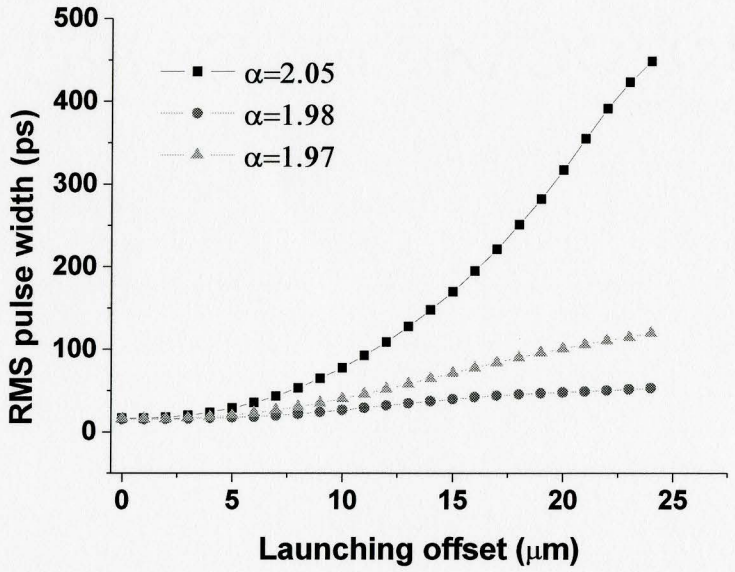

Figure4.3: RMS pulse width as a function of launching offset at different profile parameters.

Fig. 4.3 shows that under restricted launch, when the launching position is exactly at the center of the fiber core, which means no offset, DMD is minimized. This is true for $\alpha = 1.97, 1.98$ and 2.05, the reason is that, as shown in Fig. 4.4, when the launching position is located at the center of the fiber core, only a small number of lower order modes are excited and most of the power is carried by the fundamental mode, which leads to smaller DMD. Whereas, when the launching offset is getting larger, more modes are excited with more even power distribution, which leads to larger DMD.

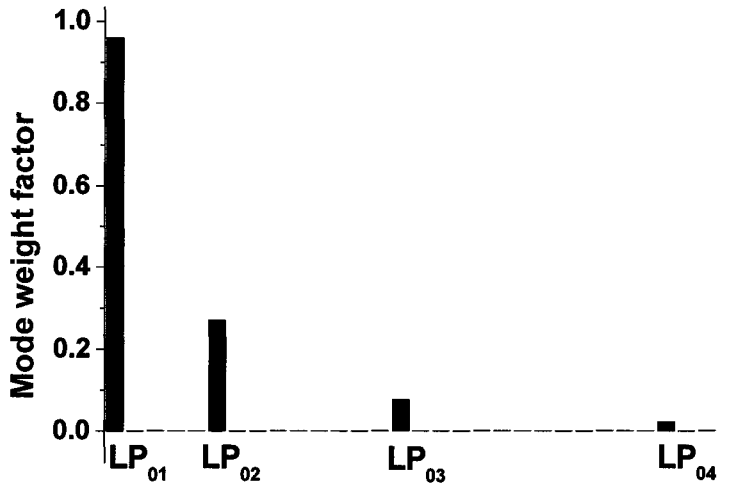
Mode weight factor
1.0
0.8
0.6
0.4
0.2
0.0
LP01
LP02
LP03
LP04

(a)

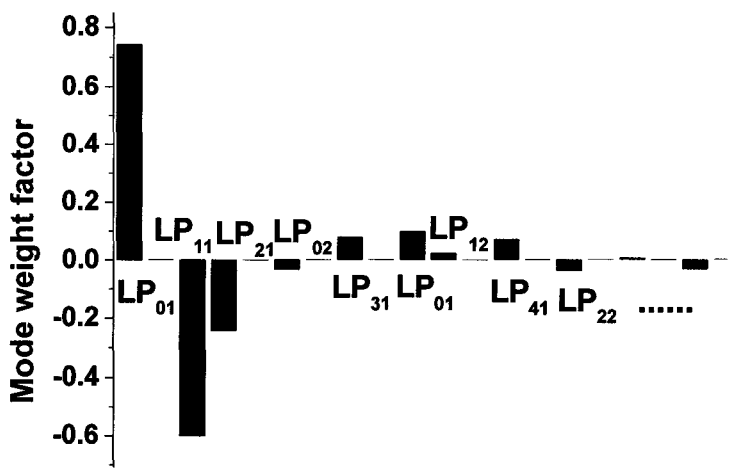
Mode weight factor
0.8
0.6
0.4
0.2
0.0
-0.2
-0.4
-0.6
LP01
LP11
LP21
LP02
LP31
LP01
LP12
LP41
LP22
.....

(b)

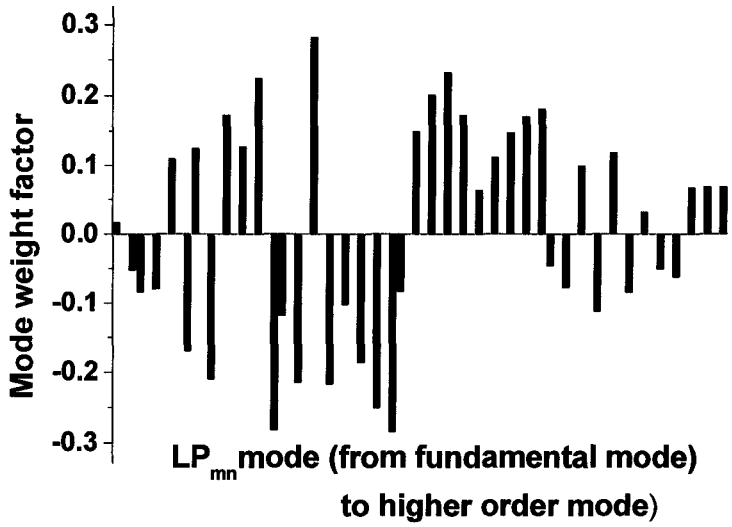

(c)

Figure4.4: Mode power distribution under restricted launch with different launching offset. (a) no offset, (b) offset= $5\mu m$ and (c) offset= $20\mu m$

4.2.3 DMD reduction using spatial filters in a 4F system

From the results in section 4.2.2, we know that DMD is smaller when there is no offset or small offset under restricted launch. This is because only a small number of lower order modes are excited and most of the power is carried by LP_{01} mode under these launching conditions. In this section, a low pass spatial filter is used in a 4F system to reduce DMD effect in a MMF under these launching conditions.

In order to understand the concept of using spatial filters to reduce DMD effect in MMFs, let us see the following example: Assuming that the output end of a fiber link is placed in

the front focal plane of the first lens (Fig. 3.2), the Fourier transform of the incident field distribution can be obtained at the back focal plane of that lens. Typically higher order modes of a MMF are rapidly varying functions along x and y directions, and therefore, they have higher spatial frequency components as compared to the fundamental mode (LP_{01}). As a result, at the back focal plane, the fundamental mode is localized to the center while the higher order modes are localized towards the edges (as shown in Fig. 4.5(b)). Therefore, a properly chosen spatial filter could alter the weight factors of modes. For example a low pass spatial filter could suppress higher order modes and a band pass spatial filter could transmit only a few selected modes. Using such a spatial filter, a large fraction of unwanted modes leading to DMD or MPI can be filtered out at the cost of losing a fraction of signal power.

As shown in Fig. 4.5, supposing that we want to keep LP_{01} mode and remove LP_{08} mode for some application. We could use a spatial filter with optimized cut-off frequency directly on the field distribution in the front focal plane of the lens (as shown in Fig. 4.5 (a)). In this case, we get a 1.9 dB power loss of LP_{08} mode, while the power loss of LP_{01} mode equals to 1 dB. However, if the spatial filter is applied to the field distribution in the back focal plane of the lens (as shown in Fig. 4.3 (b)), we can get a 9.9 dB power loss of LP_{08} mode for the same power loss of LP_{01} mode. This improvement is because the higher order mode can be further separated from the fundamental mode in the spatial frequency domain.

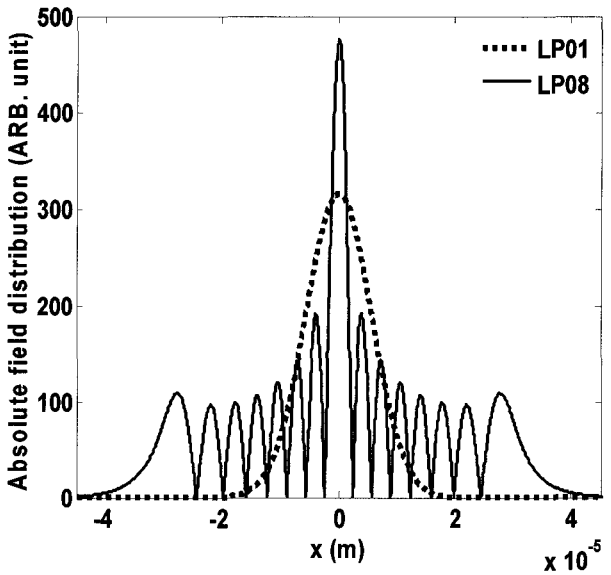

(a)

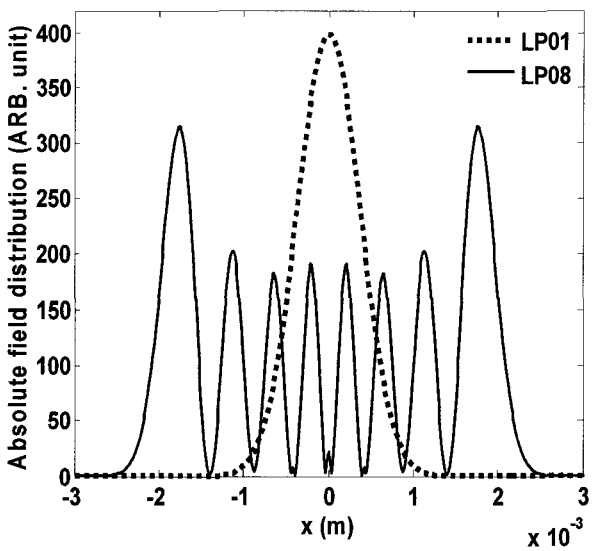

(b)

Figure4.5: (a) LP01 mode and LP08 mode distributions at the front focal plane of the first lens; (b) LP01 mode and LP08 mode distributions at the back focal plane of the first lens.

In the next simulation, a spatial filter is used in a 4F system to reduce DMD effect in MMFs under restricted launching conditions. The input signal is Gaussian shape both in time domain and spatial domain. The parameters used in the simulation are as follows: laser wavelength, 1.3 μm, core diameter, 62.5 μm, refractive index at core center, 1.491, relative refractive index difference, $\Delta = 0.01$, profile parameter of the graded index fiber, $\alpha =$ 2.05, laser spot size (FWHM)= 7 μm , and temporal pulse width (FWHM)=50 ps. In the simulation, the rms pulse width reduction is define as

$$r = \frac{\sigma_{rms1} - \sigma_{rms2}}{\sigma_{rms1}} \times 100\%, \tag{4.20}$$

where σ_{rms1} is the rms pulse width of the photo current without using spatial filter and σ_{rms2} is the rms pulse width of the photo current after using spatial filter.

In order to evaluate the performance of the proposed method, Q factor is calculated in the simulation. The Q factor is defined as

$$Q = \frac{I_1 - I_0}{\sigma_1 + \sigma_0}, \tag{4.21}$$

where I_1 and I_0 are the average values of the photo current corresponding to 1 or 0 in the On-Off keying (OOF) bit stream, σ_1 and σ_0 are the corresponding variances. The setup of the measurement is shown in Fig 4.6. The signal noise ratio (SNR) in the simulation is 10 dB.

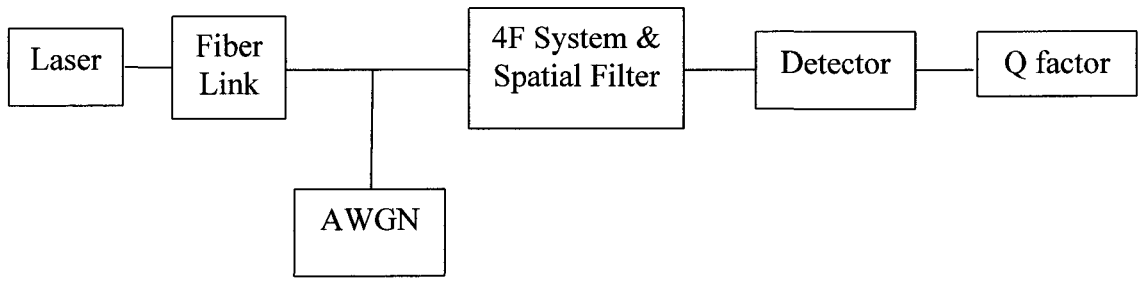

Figure4.6: The measurement setup for Q factor (AWGN: Additive White Gaussian Noise)

(1) Restricted launch using laser: no offset

As shown in Fig. 4.7, under restricted launching condition with no offset, most of the signal power is carried by LP_{01} mode. An ideal low pass spatial filter is used to remove the unwanted higher order modes. Fig. 4.7 (c) shows the reduction of mode weight factor of various LP_{mn} modes using the spatial filter. When the bandwidth of the spatial filter is equal to $76900\,m^{-1}$, from Fig. 4.7 (d) we see that the rms pulse width is reduced from 67.8 ps to 27.9 ps after a propagation distance of 10 Km, while the power loss of the signal is only 0.99 dB, as shown in Fig. 4.7(a).

In this example, the power loss due to MMF and spatial filter is not a serious problem since the propagation distance is quiet short (≤ 10 Km) and therefore, the optimum bandwidth of spatial filter as shown in Fig 4.6 (a) needs not to be the optimum bandwidth. In fact, from Fig 4.7 (b), the optimum bandwidth is $46200m^{-1}$.

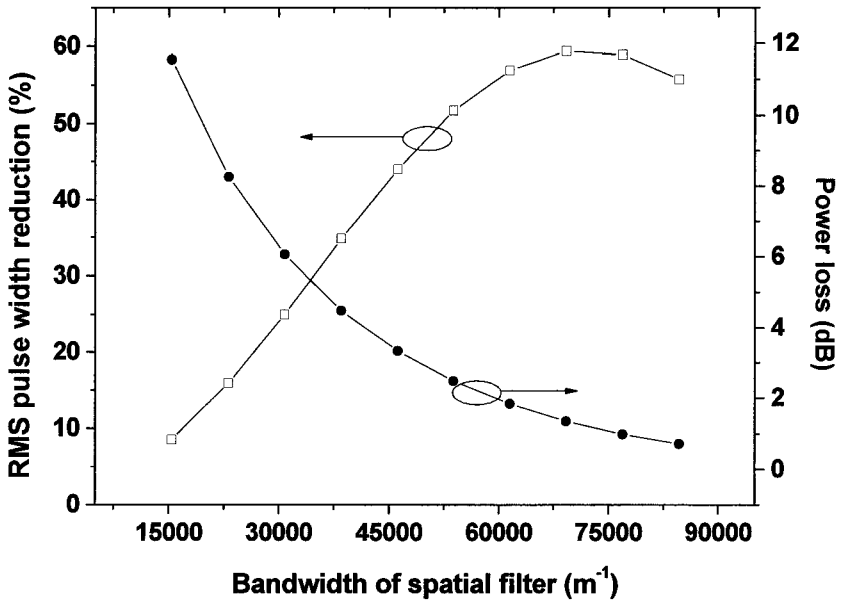
RMS pulse width reduction (%)
Power loss (dB)
Bandwidth of spatial filter (m-1)
0
10
20
30
40
50
60
0
2
4
6
8
10
12
15000
30000
45000
60000
75000
90000

(a)

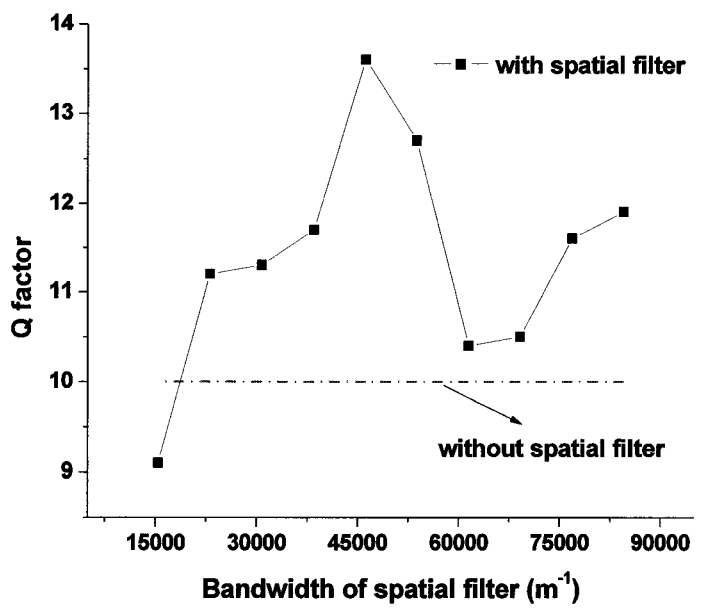
Q factor
Bandwidth of spatial filter (m-1)
with spatial filter
without spatial filter
9
10
11
12
13
14
15000
30000
45000
60000
75000
90000

(b)

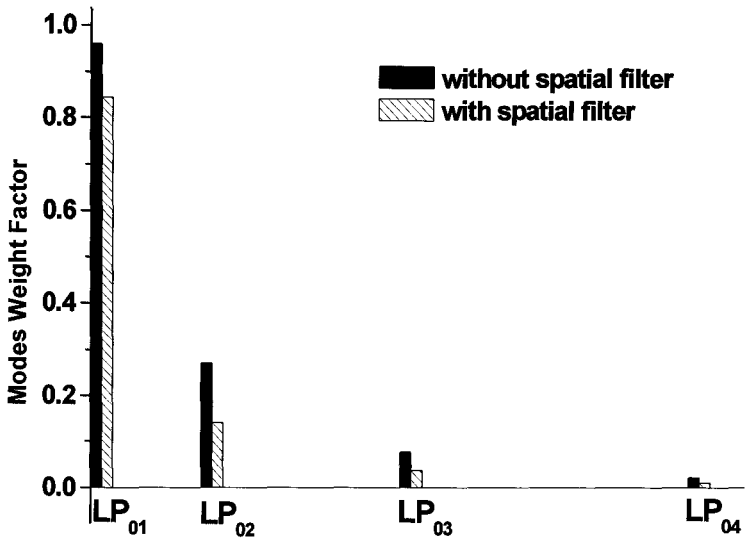
1.0
0.8
0.6
0.4
0.2
0.0
Modes Weight Factor
without spatial filter
with spatial filter
LP01
LP02
LP03
LP04

(c)

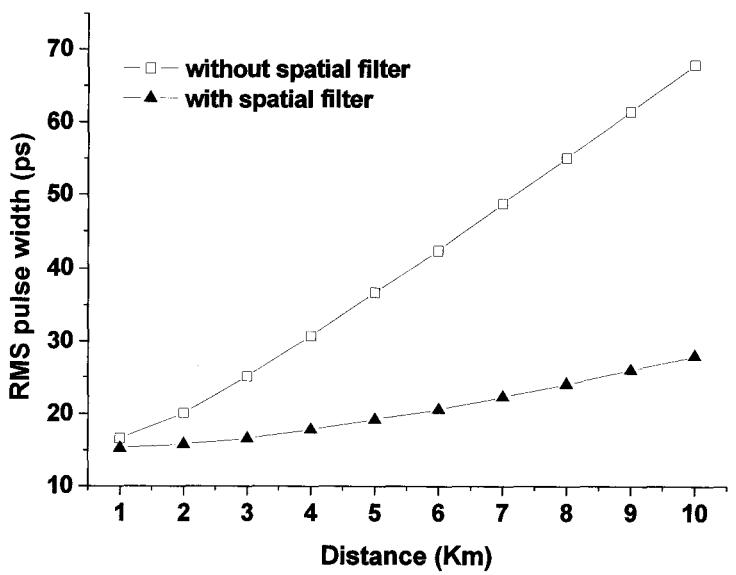
70
60
50
40
30
20
10
RMS pulse width (ps)
without spatial filter
with spatial filter
1
2
3
4
5
6
7
8
9
10
Distance (Km)

(d)

Figure4.7: (a) rms pulse width reduction and power loss as a function of the bandwidth of the spatial filter at 10 Km, (b) Q factor as a function of the spatial filter at 10Km, (c) modes weight distribution when the bandwidth of the spatial filter is equal to $76900\,m^{-1}$, (d) rms pulse width as a function of propagation distance when the bandwidth of the spatial filter is equal to $76900\,m^{-1}$.

(2) Restricted launch using laser: offset=5 μm

As shown in Fig.4.8, under restricted launching condition with 5 μm offset, most of the signal power is carried by lower order modes (LP_{01}, LP_{11}, and LP_{21}). An ideal low pass spatial filter is used to remove unwanted higher order modes other than LP_{01}, LP_{11} and LP_{21}. When the cutoff frequency of the spatial filter is equal to $84600\,m^{-1}$, from Fig. 4.8 (c) we see that the rms pulse width is reduced from 196 ps to 160 ps after a propagation distance of 10 Km, while the power loss of the signal is 1.21 dB. In this case, the rms pulse width reduction is not so much as in the case of restricted launch condition with no offset. This is because that the signal power is distributed more evenly among more modes in this case. A low pass spatial filter can not be used to effectively reduce the DMD effect.

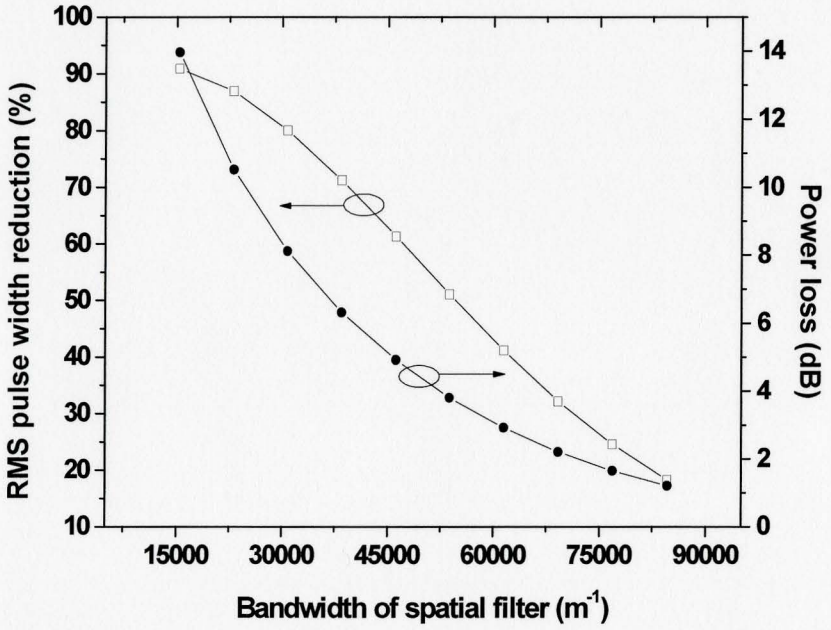
RMS pulse width reduction (%)
Power loss (dB)
Bandwidth of spatial filter (m-1)
100
90
80
70
60
50
40
30
20
10
14
12
10
8
6
4
2
0
15000
30000
45000
60000
75000
90000

(a)

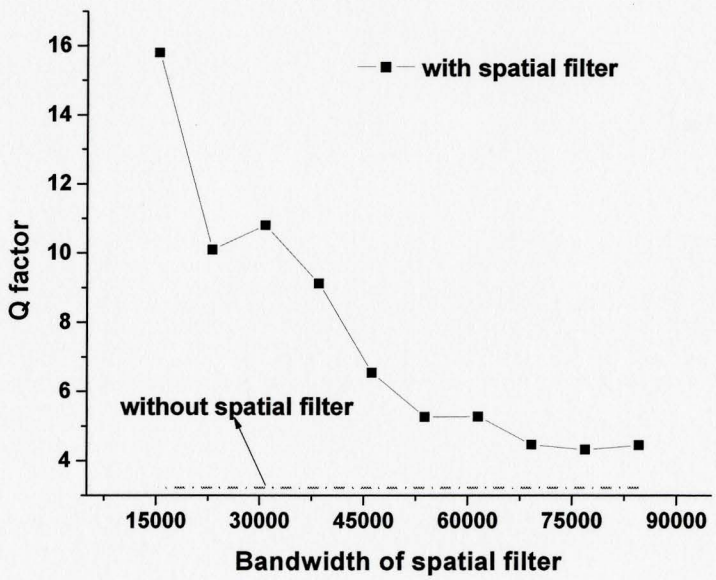
with spatial filter
without spatial filter
Q factor
Bandwidth of spatial filter
16
14
12
10
8
6
4
15000
30000
45000
60000
75000
90000

(b)

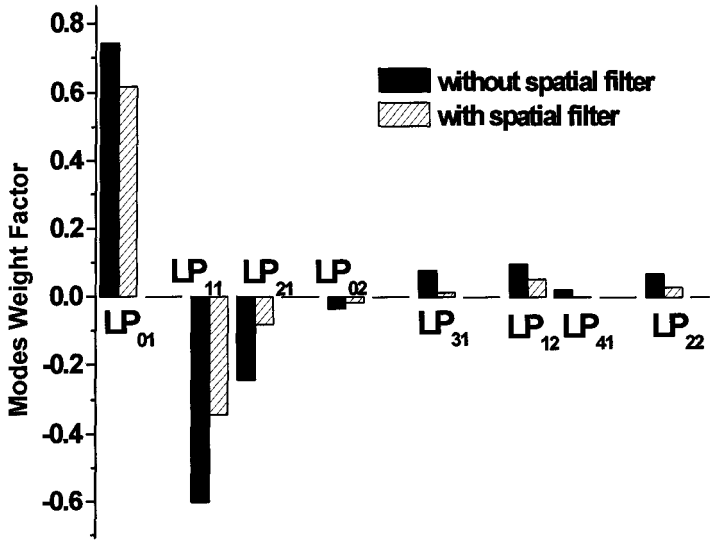
0.8
0.6
0.4
0.2
0.0
-0.2
-0.4
-0.6
Modes Weight Factor
without spatial filter
with spatial filter
LP01
LP11
LP21
LP02
LP31
LP12
LP41
LP22

(c)

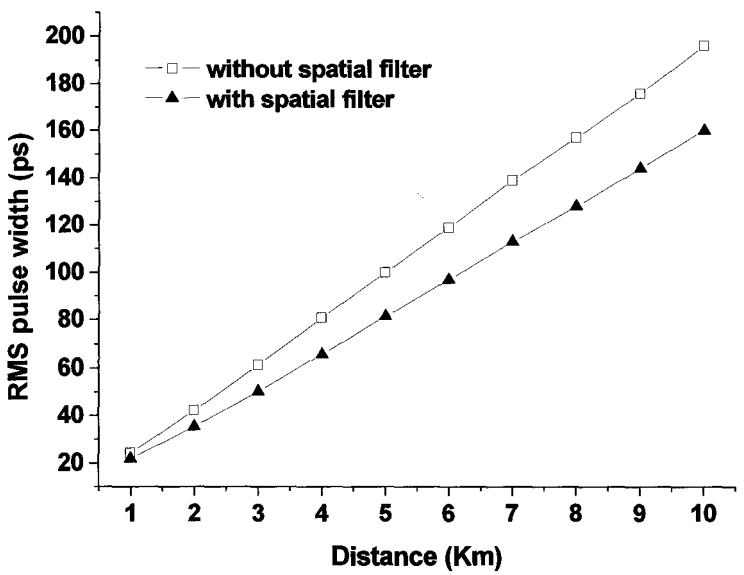
200
180
160
140
120
100
80
60
40
20
RMS pulse width (ps)
without spatial filter
with spatial filter
1
2
3
4
5
6
7
8
9
10
Distance (Km)

(d)

Figure4.8: (a) rms pulse width and power loss as a function of the bandwidth of the spatial filter at 10 Km, (b) Q factor as a function of the spatial filter at 10Km, (c) modes weight distribution when the bandwidth of the spatial filter is equal to $84600\,m^{-1}$, (d) rms pulse width as a function of propagation distance when the bandwidth of the spatial filter is equal to $84600\,m^{-1}$.

In the above simulations, the wavelength of the input light is $1.3\,\mu m$, the focal length of the lens is $1\,cm$, so the bandwidths of the spatial filter in spatial frequency, $76900\,m^{-1}$ and $84600\,m^{-1}$, correspond to $1\,mm$ and $1.1\,mm$ in spatial dimension, respectively. If lenses with much larger focal length are used, the bandwidths of the spatial filter could be made even larger, which is easier to implement in experiment.

4.3 MPI reduction using spatial filters

4.3.1 Mathematical analysis of MPI in a few mode fibers

In a few mode fibers, signal travels in fundamental mode (LP_{01} mode), a higher order mode (LP_{11} or LP_{02}) travels as a weak replica. Supposing that at the output of the fiber, the peak electric field amplitude of the fundamental mode is E_1 and the peak electric field amplitude of the higher order mode is E_2. At the receiver, the output signal is given by

$$S_o = |E_1 + E_2|^2 = |E_1|^2 + E_1 E_2^* + E_1^* E_2 + |E_2|^2 \tag{4.22}$$

The term $E_1E_2^* + E_1^*E_2$ is responsible for the interference pattern at the receiver. MPI is defined as

$$MPI(dB) = 10\log_{10}\frac{P_2}{P_1} \tag{4.23}$$

where P_1 ($\propto |E_1|^2$) is the power of the fundamental mode and P_2 ($\propto |E_2|^2$) is the power of the higher order mode.

4.3.2 MPI reduction using spatial filters in a 4F system

As discussed in section 4.2.3, higher order modes have higher spatial frequency components. At the back focal plane of a lens, they can be partially separated from fundamental mode using a spatial filter. In this section, specially designed filters are utilized in a 4F system to reduce MPI in a few mode fibers by suppressing unwanted higher order modes. Two situations are investigated

(1) Signal propagates in LP_{01} mode and LP_{11} mode acts as a weak replica.

(2) Signal propagates in LP_{01} mode and LP_{02} mode acts as a weak replica.

In the simulation, in order to quantify the reduction of MPI, MPI reduction factor is defined as

$$\alpha(dB) = MPI(dB)_{input} - MPI(dB)_{output}. \tag{4.24}$$

where $MPI(dB)_{input}$, $MPI(dB)_{output}$ are MPI in dB unit at the input and the output of the 4F systems, respectively.

First, we consider MPI in a twin mode fiber. In order to simulate MPI reduction in LP_{01} mode and LP_{11} mode case, a step index SMF with the following parameters is used: core radius of the fiber is $4.2\,\mu m$, core refractive index of the fiber n_1 is 1.46, cladding refractive index n_2 is 1.45562, and the cutoff wavelength is $1.24\,\mu m$. This fiber supports LP_{01} mode and LP_{11} mode at a laser wavelength of $0.8\,\mu m$.

The mode amplitude contour diagrams for LP_{01} mode and LP_{11}mode at the front focal plane of the first lens are illustrated in Fig. 4.9(a), whereas the Fourier Transform of these two modes at the back focal plane of the first lens are shown in Fig. 4.9 (b). It is found that if a spatial filter is used at the front focal plane, the MPI reduction factor is much less than that if the spatial filter is used at the back focal plane, which can also be observed in Fig. 4.9. It is apparently that these two modes are more separated from each other after the Fourier Transform is performed. So if a properly chosen spatial filter is utilized, a large fraction of LP_{11} mode could be filtered out. As a result, MPI can be reduced at the cost of losing some power of LP_{01} mode.

If a spatial filter (as shown by the dashed line in Fig. 4.9 (b)) is used to let the central part of the signal pass, and let the other part of the signal stop, a large fraction of LP_{11} mode can be removed, leading to MPI reduction. As shown in Fig. 4.10, when the bandwidth of the spatial filter decreases from $8.37 \times 10^4\ m^{-1}$ to $0.56 \times 10^4\ m^{-1}$ (from

670 μm to 44.8 μm), the MPI reduction factor is increased from 6 dB to more than 26 dB, while the power loss of LP_{01} mode is increased from 1.7 dB to 11.7 dB. Thus, there is a trade-off between the power loss of LP_{01} mode and MPI reduction factor.

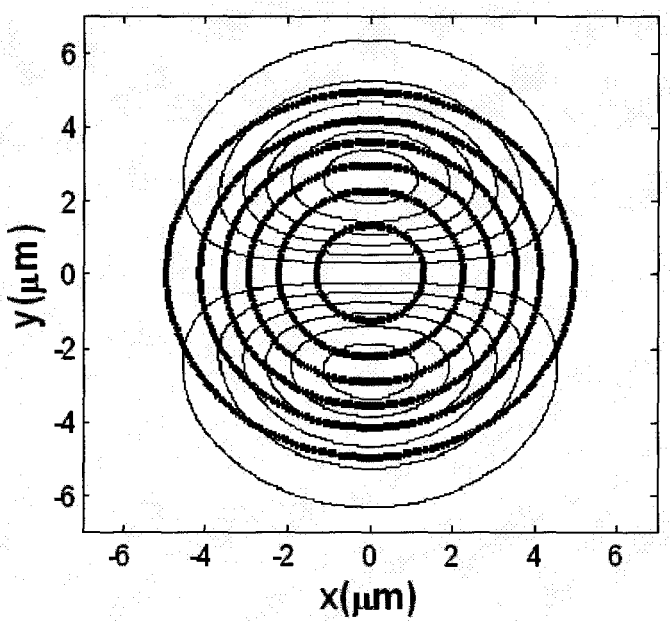

(a)

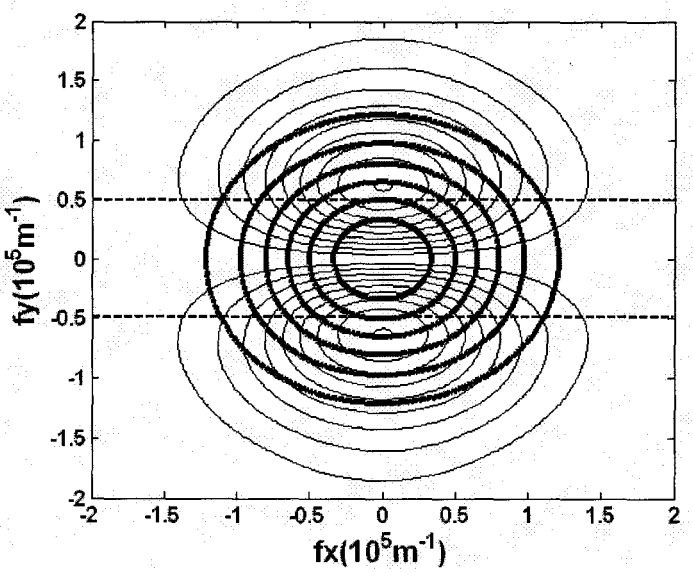

(b)

Figure4.9: (a) Mode amplitude contour diagrams for LP01 mode and LP11mode at the front focal plane of the first lens; (b) Fourier Transform of the LP01 mode and LP11mode at the back focal plane of the first lens. Thick line: LP01 mode, thin line: LP11 mode, dash line: central pass filter.

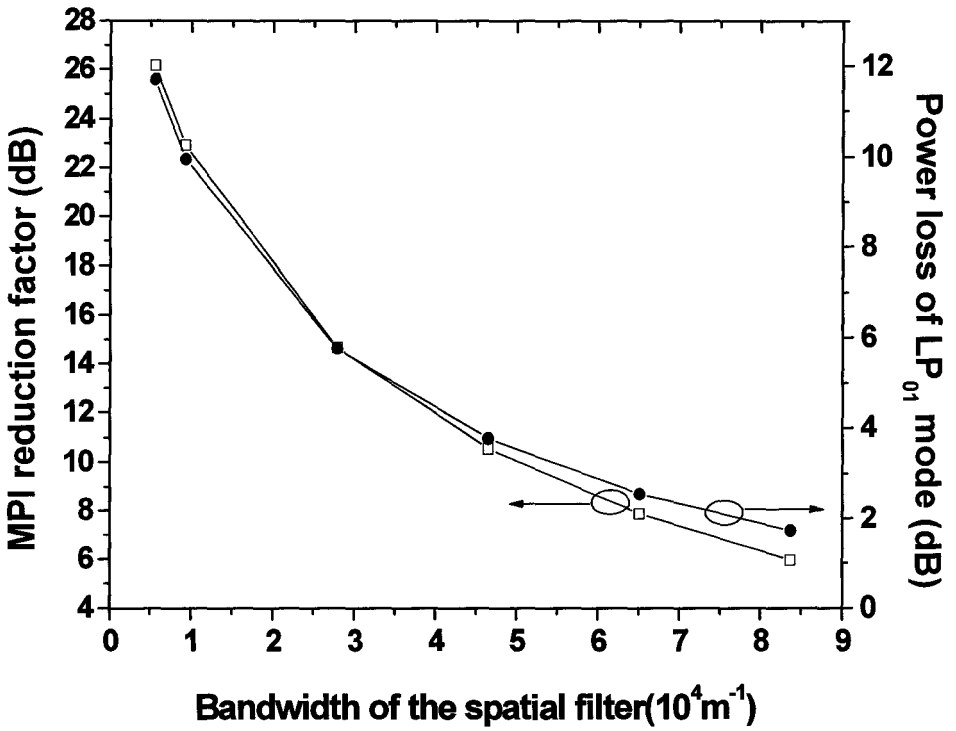

Figure4.10: Power loss and MPI reduction after using spatial filter for LP01 mode and LP11 mode case

Next we consider the case of coupling between LP_{01} mode and LP_{02} mode. In this case, signal travels in LP_{01} mode and LP_{02} mode is the weak replica (as in HOM-DCF). In this example, the parameters of the fiber are the same as that in the above example. The wavelength of the laser is set to be $0.5\,\mu m$ so that the fiber can support LP_{01} mode and LP_{02} mode.

The mode amplitude contour diagrams for LP_{01} mode and LP_{02} mode at the front focal plane of the first lens and their Fourier Transforms at the back focal plane of the first lens are shown in Fig. 4.11 (a), (b), respectively. Again, it is observed that the amplitude distributions of these two modes are almost overlapped at the input of a 4F system (Fig. 4.11 (a)), whereas they can be partially separated after the Fourier Transform is performed (Fig.4.11 (b)). So a circular low pass spatial filter could be used to suppress some fraction of LP_{02} mode to reduce MPI effects.

As shown in Fig. 4.12, when the bandwidth of the low pass spatial filter is increased from $1.25\times10^4\,m^{-1}$ to $6.25\times10^4\,m^{-1}$ (from $62.5\,\mu m$ to $313\,\mu m$), the MPI reduction factor is increased from 4 dB to about 8 dB. In this case, even when the MPI reduction factor is $8\,dB$, the power loss of LP_{01} mode is quite small ($\approx 1\,dB$).

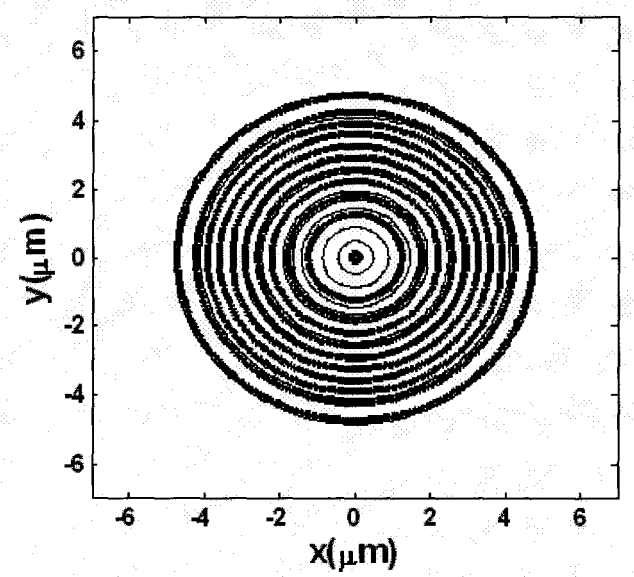

(a)

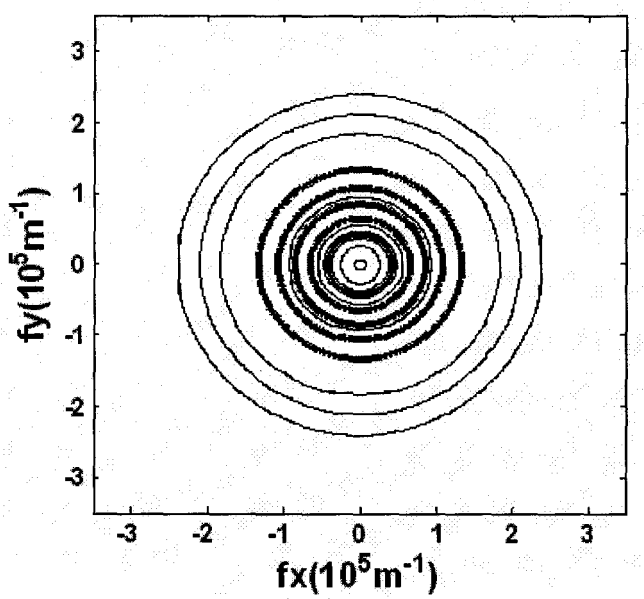

(b)

Figure4.11: (a) Mode amplitude contour diagrams for LP01 mode and LP02 mode at the front focal plane of the first lens, (b) Fourier Transform of the LP01 mode and LP02 mode at the back focal plane of the first lens. Thick line: LP01 mode, thin line: LP02 mode.

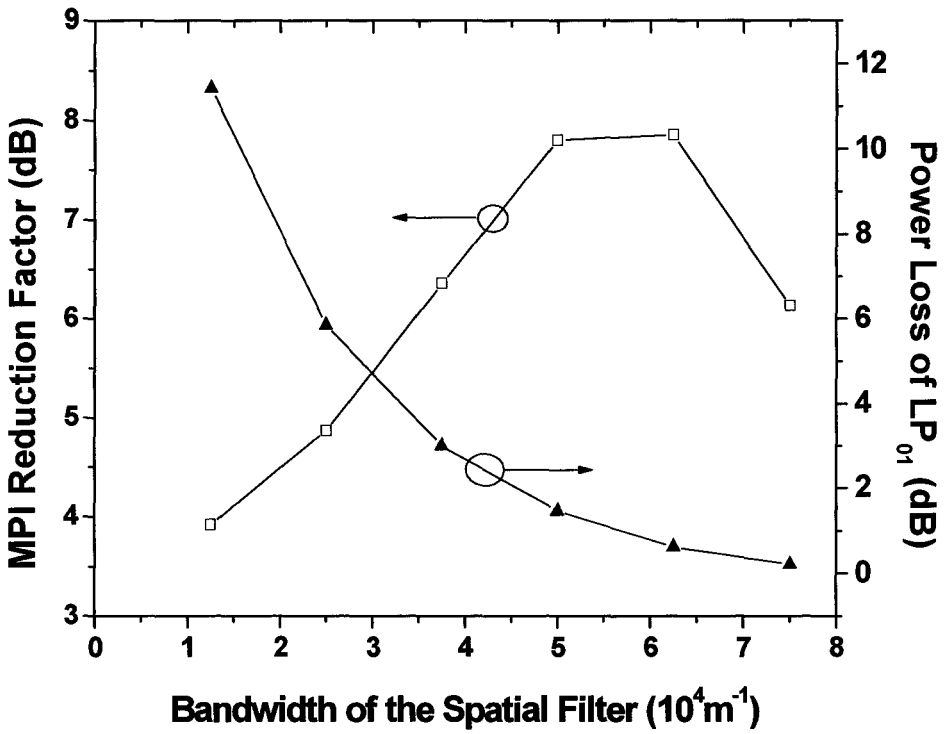

Figure4.12: Power loss and MPI reduction after using spatial filter for LP01 mode and LP02 mode case

4.4 Conclusion

In this chapter, we have shown that the effects of MPI and DMD can be reduced using spatial filters in the 4F system. Higher order modes have higher spatial frequency components and therefore, they are spatially separated from the fundamental mode at the back focal plane of the

Lens 1. By optimizing the spatial filter bandwidth, unwanted higher order modes can be suppressed.

Our simulation results have shown that, for the reduction of DMD effect, the rms pulse width broadening factor can be reduced up to 58.9% with only 0.99 dB power loss of the signal for the case of restricted launch with no offset. For the case of MPI reduction, two cases have been investigated: firstly, signal propagates in LP_{01} mode and LP_{11} mode acts as a weak replica; secondly, signal propagates in LP_{01} mode and LP_{02} mode acts as a weak replica. For the first case, the simulation results shown that using a properly chosen spatial filter, the MPI reduction factor is 6 dB when the power loss of LP_{01} mode is 1.7 dB. The MPI reduction factor can be further increased to 26 dB at the cost of increased power loss of LP_{01} mode. For the second case, the simulation results shown that an optimum bandwidth of the low pass spatial filter can be found to obtain a MPI reduction factor of 8 dB with 1 dB power loss of Lp_{01} mode.

Chapter 5

Tunable Optical Filters Using Temporal Filtering

5.1 Introduction

Tunable optical filters are important devices in WDM systems which are used to select a particular wavelength dynamically at the add-drop nodes. Tunable optical filters are typically implemented using Fabry-Perot (FP) interferometer, Mach-Zehnder (MZ) interferometer, fibre Bragg grating and acousto-optic Filter [25-27]. In this chapter, we propose to implement the tunable optical filters using time lenses and single mode fibers. A time lens is actually a phase modulator which introduces a quadratic phase factor in time domain. Using single mode fibers and time lenses, a temporal 4F system can be established to perform temporal filtering with a temporal filter. The output bit pattern of this 4F system is reversed in time compared with the input bit pattern of the 4F system [24]. In this chapter, we propose a new configuration that the output bit pattern is not reversed in time. So no extra signal processing components are needed following the 4F system. We believe that this new scheme can be used as a tunable optical filter in WDM systems.

5.2 Tunable optical filter using modified temporal 4F system

Let us consider a modified temporal 4F system as shown in Fig. 5.1. Compared to Fig. 3.4, we see that the sign of the voltage of the time lens and dispersion coefficient of the

signal mode fibers in the second temporal 2F system are both changed, which are opposite to those of the first temporal 2F system.

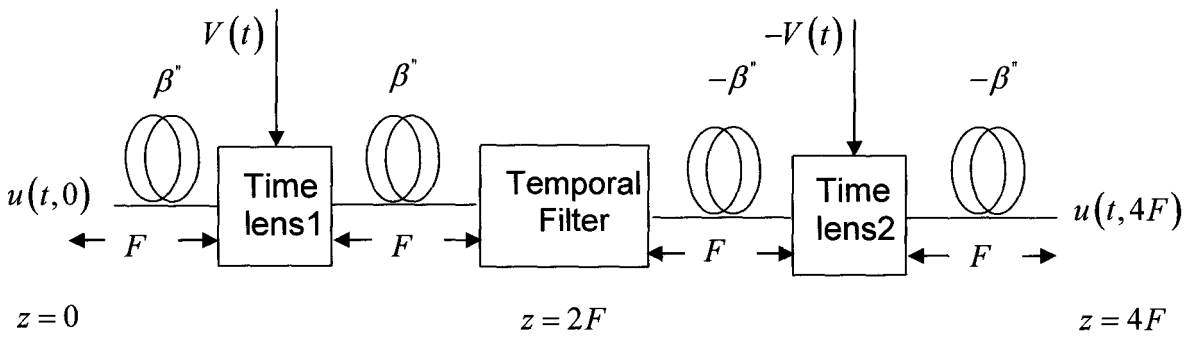

Figure5.1: Modified 4F system using SMFs and time lens

Assuming the signal at the back focal plane of the first time lens is $u(t,2F)$, its Fourier transform is given by

$$\tilde{u}(\omega,2F)=\int_{-\infty}^{\infty}u(t,2F)\exp(j\omega t)dt \tag{5.1}$$

The signal immediately before the second time lens is given by

$$\tilde{u}(\omega,3F_{-})=\tilde{u}(\omega,2F)\exp\left(-\frac{j\beta^{"}F\omega^{2}}{2}\right) \tag{5.2}$$

From Eq. (3.21), we have

$$u(t,2F)=\tilde{u}(\omega,F_{+})\exp\left(\frac{j\beta^{"}F\omega^{2}}{2}\right) \tag{5.3}$$

Substituting Eq. (5.3) into Eq. (5.2), we obtain

$$\tilde{u}(\omega, 3F_-) = \tilde{u}(\omega, F_+) \tag{5.4}$$

So we can get

$$u(t, 3F_-) = u(t, F_+) \tag{5.5}$$

The signal immediately after the second time lens is given by

$$u(t, 3F_+) = u(t, 3F_-)\exp(-j\xi\alpha t^2) \tag{5.6}$$

where ξ and α are defined in chapter 3. Substituting Eq. (5.5) into Eq. (5.6), we obtain

$$u(t, 3F_+) = u(t, F_+)\exp(-j\xi\alpha t^2) \tag{5.7}$$

The relationship between the signals immediately before and after the first time lens is given by

$$u(t, F_+) = u(t, F_-)\exp(j\xi\alpha t^2) \tag{5.8}$$

Substituting Eq. (5.8) into Eq. (5.7), we obtain

$$u(t, 3F_+) = u(t, F_-) \tag{5.9}$$

and

$$\tilde{u}(\omega, 3F_+) = \tilde{u}(\omega, F_-) \tag{5.10}$$

The signal at the output of the 4F system is given by

$$\tilde{u}(\omega,4F)=\tilde{u}(\omega,3F_{+})\exp\left(-\frac{j\beta^{''}F\omega^{2}}{2}\right) \tag{5.11}$$

Substituting Eq. (5.10) into Eq. (5.11), we obtain

$$\tilde{u}(\omega,4F)=\tilde{u}(\omega,F_{-})\exp\left(-\frac{j\beta^{''}F\omega^{2}}{2}\right) \tag{5.12}$$

From Eq. (3.19), we have

$$\tilde{u}(\omega,F_{-})=\tilde{u}(\omega,0)\exp\left(\frac{j\beta^{''}F\omega^{2}}{2}\right) \tag{5.13}$$

Substituting Eq. (5.13) into Eq. (5.12), we obtain

$$\tilde{u}(\omega,4F)=\tilde{u}(\omega,0) \tag{5.14}$$

and

$$u(t,4F)=u(t,0) \tag{5.15}$$

Finally, we can see that the output signal of the modified 4F system without using temporal filters is exactly the same as the input signal. Under this configuration, the time reversal is removed. The tunable optical filter can be implemented using this configuration with a temporal filter.

As an example, let us consider the case of a 2 channels WDM system operating at 40 Gb/s/channel with a channel separation of 200 GHz. Let the input to the 4-f system shown in Fig. 5.2 be the superposition of two channels. In this example, we have simulated a random bit pattern consisting of 16 bits in each channel. The data '1' is

represented by a Gaussian pulse of width 12.5 ps. Focal length F of the time lens = 1 km and $\beta^{''}$ = 5 ps^2/km. The temporal filter is realized using an amplitude modulator with a time-domain transfer function

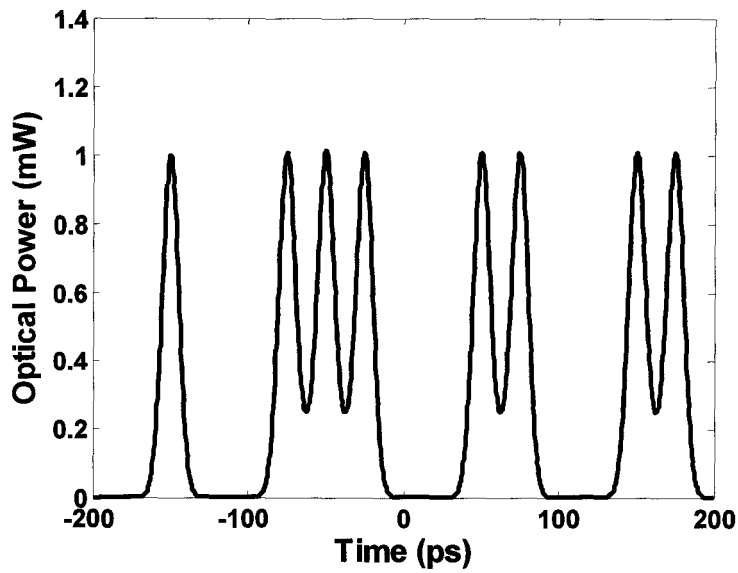

(a)

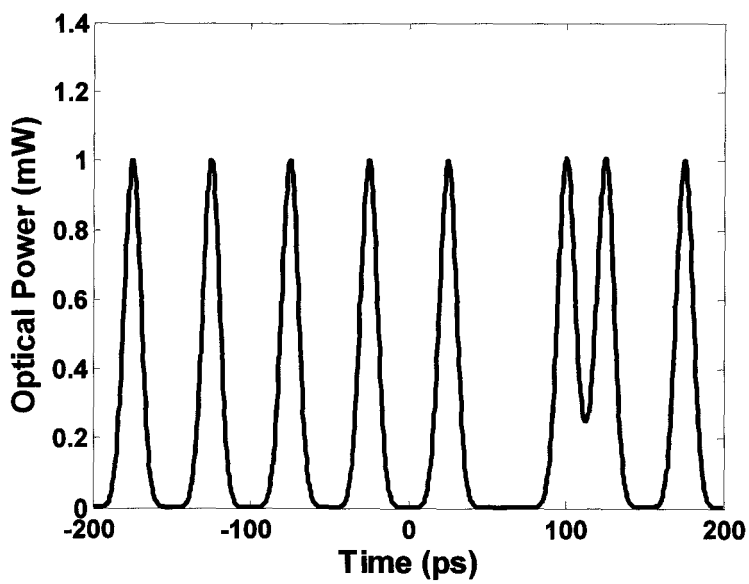

(b)

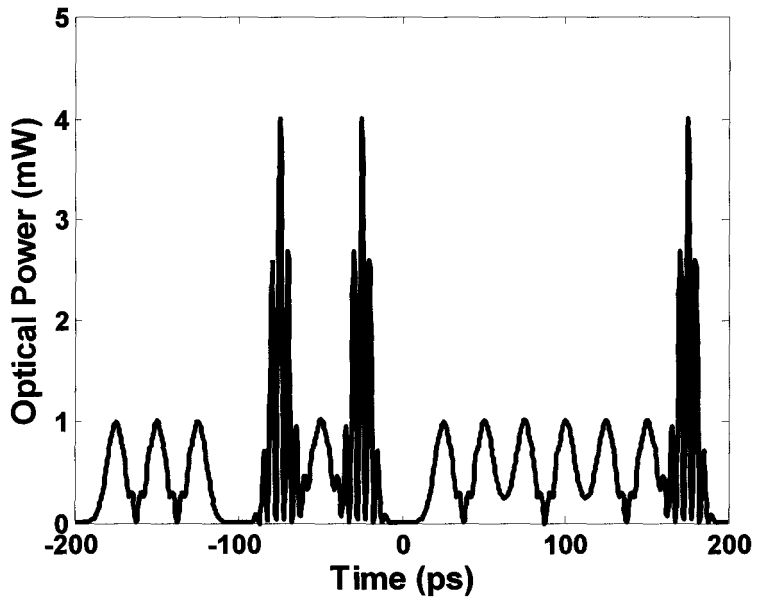
Optical Power (mW)
Time (ps)
5
4
3
2
1
0
-200
-100
0
100
200

(c)

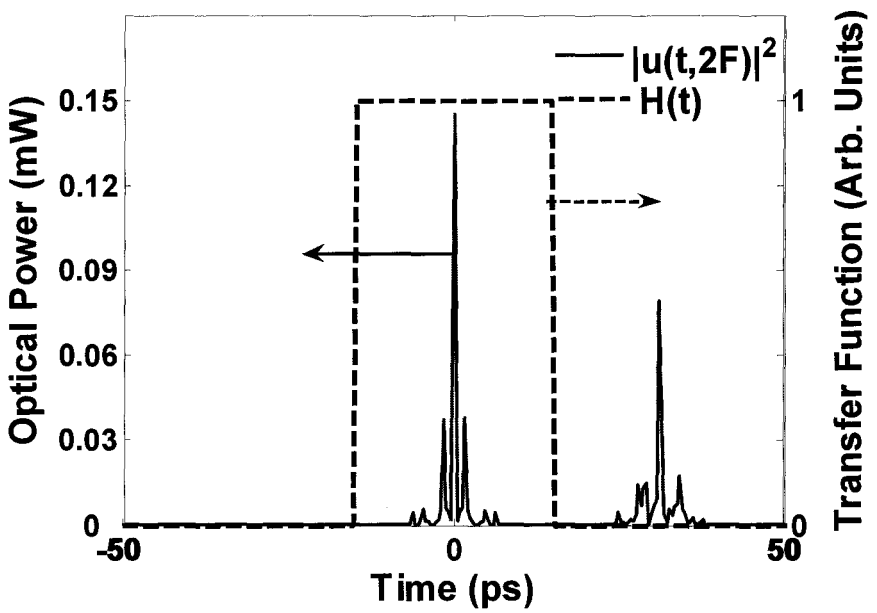
|u(t,2F)|2
H(t)
Optical Power (mW)
Transfer Function (Arb. Units)
Time (ps)
0.15
0.12
0.09
0.06
0.03
0
1
0
-50
0
50

(d)

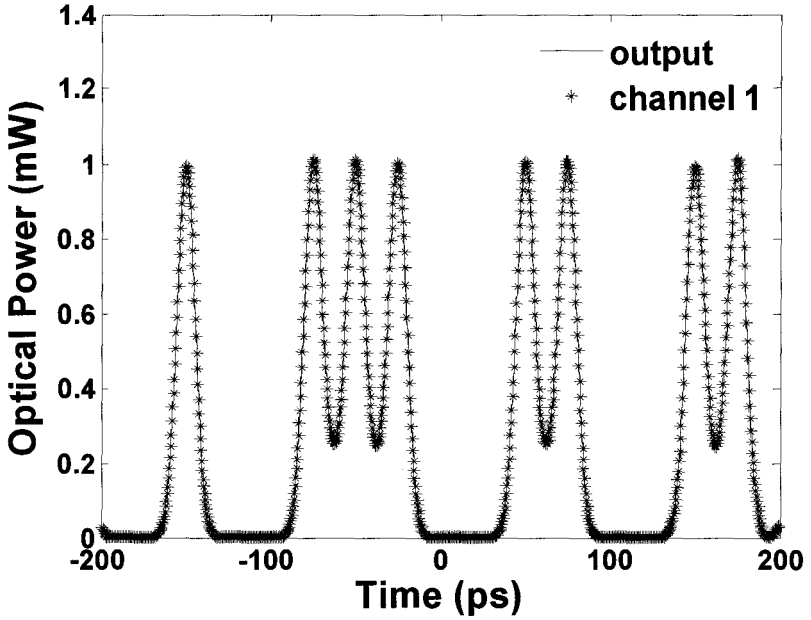

(e)

Figure5.2: (a) Signal power of channel 1; (b) Signal power of channel 2; (c) Multiplexed signal power at $z = 0$; (d) Signal power at $z = 2F$; (e) signal power at $z = 4F$.

$$H(t) = 1 \quad \text{if } |t| \leq t_c$$
$$= 0 \quad \text{otherwise} \tag{5.16}$$

where t_c = 15 ps so that channel 1 is transmitted and channel 2 is blocked. Fig. 5.2 (a) shows the power distribution just before the temporal filter which is the absolute square of the Fourier transform of the signal incident on the modified 4F configuration. Solid line in Fig.5.2 (b) shows the output of the modified 4F system while '*' shows the input bit pattern of channel 1 before multiplexing. As can be seen, the data in channel 1 can be successfully demultiplexed. The advantage of the proposed scheme is that the channels

to be demultiplexed at a node can be dynamically reconfigured. For example, if channel 1 has to be blocked instead of channel 2, the transmittivity of the amplitude modulator (Eq.5.16) can be dynamically changed to

$$H(t) = 0 \quad \text{if } |t| \leq t_c$$
$$= 1 \quad \text{otherwise} \tag{5.17}$$

As shown in Fig.5.3, the data in channel 2 can be successfully demultiplexed.

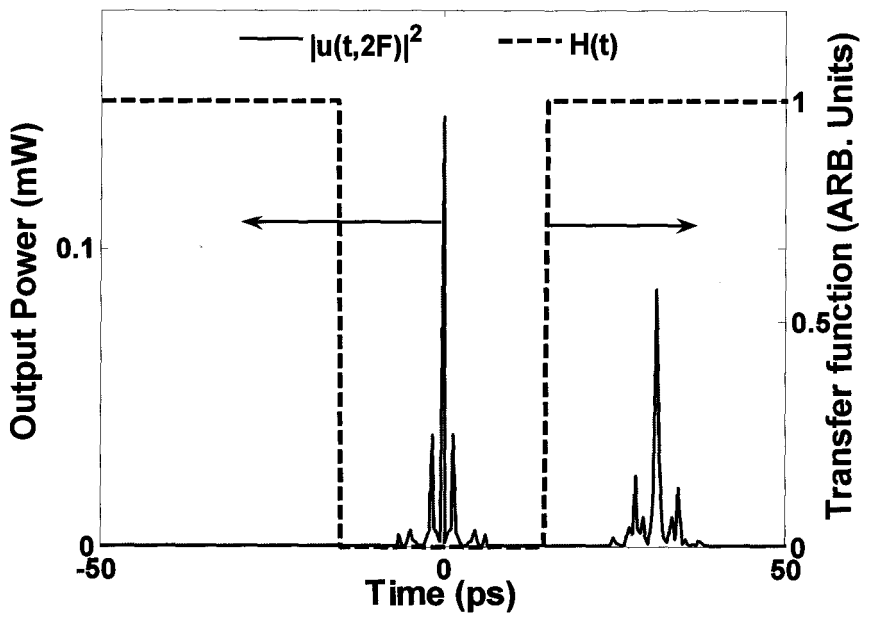

(a)

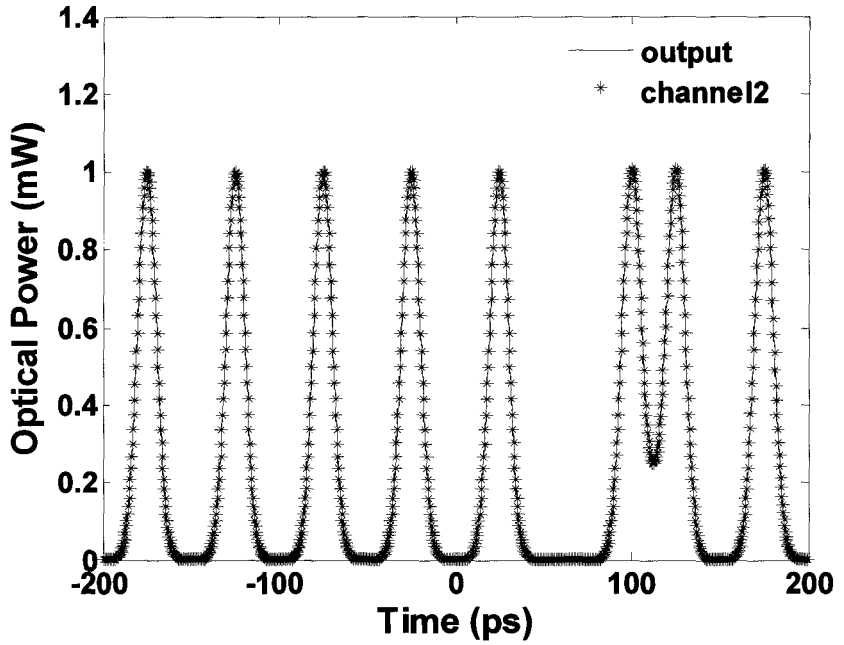

(b)

Figure5.3: (a) Signal power at $z = 2F$; (b) signal power at $z = 4F$.

5.3 Conclusion

In this chapter, a modified 4F system using SMFs and time lens was proposed and analyzed. The application of using temporal filtering to implement tunable optical filter was proposed. Simulation results have shown that using this modified 4F system with a temporal filter, a tunable optical filter could be implemented to demultiplex signals in WDM systems.

Chapter 6

Conclusions

Differential mode delay (DMD) and multipath interference (MPI) are dominant impairments in MMF transmission system. In this thesis, mathematical analysis of DMD in MMF under restricted launching conditions and MPI is carried out. A method to suppress DMD and MPI based on spatial filtering in a 4F system is proposed. Higher order modes have higher spatial frequency components and therefore, they are spatially separated from the fundamental mode at the back focal plane of the first lens of the 4F system. By optimizing the spatial filter bandwidth, unwanted higher order modes can be suppressed.

Our simulation results have shown that using spatial filters in a 4F system, DMD effects can be reduced. Under restricted launching condition with no offset, rms pulse width can be reduced up to 58.9% with only 0.99 dB power loss of the signal using a low pass spatial filter. MPI can also be reduced using this method. As the MPI reduction factor increases, the signal power loss also increases and thus, there is a trade off between the two. By optimizing the spatial filter bandwidth, MPI reduction factor can be as large as 8 dB, while the power loss of LP_{01} mode is about 1 dB.

A method using temporal filtering technique to implement tunable optical filter is also proposed in this thesis. The modified configuration of 4F system using time lens and SMF is introduced. Using this modified configuration, the output temporal signal of the 4F system is not time reversed. So there is no need for additional signal processing in optical or electrical domain to recover the original bit sequence. Simulation results have shown that this configuration can be used as a tunable optical filter to demultiplex signals in WDM systems.

Bibliography

[1] A. Ghatak and K. Thyagarajan, *Optical Electronics*, Cambridge University Press, 1989

[2] L. Raddatz, I. H. White, D. G. Cunningham and M. C. Nowell, "Increasing the bandwidth-distance product of multimode fiber usingoffset launch," Electron. Lett., vol. 33, pp. 232–233, 1997.

[3] L. Raddatz, I. H. White, D. G. Cunningham and M. C. Nowell, "An Experimental and Theoretical Study of the Offset Launch Technique for the Enhancement of the Bandwidth of Multimode Fiber Links," J. of Lightwave Technol. vol. 16,324-331, 1998

[4] G. P. Agrawal, *Fiber-Optic Communication Systems*, second edition, John Wiley & Sons Inc, 1997

[5] N. Guan, K. Takenaga, S. Matsuo and K. Himeno, "Multimode Fibers for Compensating Intermodal Dispersion of Graded-Index Multimode Fibers," J. Lightwave Technol. 7, 1719-1714, 2004.

[6] L. Raddatz, I. H. White, D. G. Cunningham and M. C. Nowell, "Increasing the bandwidth-distance product of multimode fiber using offset launch," Electron. Lett. 3, 232–233, 1997.

[7] C.-A. Bunge, S. Choi and K. Oh, "Analysis of ring launching scheme using hollow optical fibre mode converter for 10 Gbps multimode fibre communication," Optical Fiber Technol. 1, 48-58, 2006.

[8] X. Zhao and F. S. Choa, "Demonstration of 10-Gb/s Transmissions Over a 1.5-km-Long Multimode Fiber Using Equalization Techniques," IEEE Photon. Technol. Lett. 8, 1187-1189, 2002.

[9] K. M. Patel, A. Polley, K. Balemarthy and S. E. Ralph, "Spatially Resolved Detection and Equalization of Modal Dispersion Limited Multimode Fiber Links," J. Lightwave Technol. 7, 2629-2636, 2006.

[10] C. Argon, K. M. Patel, S. W. McLaughlin and S. E. Ralph, "Exploiting Diversity in Multimode Fiber Communications Links Via Multisegment Detectors and Equalization," IEEE Communications Lett.8, 400-402, 2003.

[11] C. R. S. Fludger and R. J. Mears, "Electrical measurements of multipath interference in distributed Raman amplifiers," J. Lightwave Technol. 4, 536–545, 2001.

[12] C. X. Yu, W.K. Wang and S. D. Brorson, "System degradation due to multipath coherent crosstalk in WDM network nodes," J. Lightwave Technol. 8, 1380–1386, 1998.

[13] J. L. Gimlett and N. K. Cheung, "Effects of phase-to-intensity noise conversion by multiple reflections on gigabit-per-second DFB laser transmission systems," J. Lightwave Technol. 6, 888–895, 1989.

[14]Y. Liu, "Large effective area waveguide fiber," US Patent 5835655, 1998.

[15] S. Ramachandran, J.W. Nicholson, S. Ghalmi and M. F.Yan, "Measurement of multipath interference in the coherent crosstalk regime," IEEE Photon. Technol. Lett. 8, 1171–1173, 2003.

[16] Y. Danziger, E. Herman, U. Levy and M. Rosenblit, "Reducing mode interference in transmission of LP02 Mode in optical fibers," US Patent 6,327,403, 2001.

[17] J. W. Goodman, *Introduction to Fourier Optics*, McGraw-Hill, 1968.

[18] S. Cherukulappurath, G. Boudebs and A. Monteil, "4f coherent imager system and its application to nonlinear optical measurements", J. Opt. Soc. Am. B, 21, 273-279 2004.

[19] J. L. Horner, "Joint transform correlator using a 4-F lens system to achieve virtual displacement along the optical axis," US Patent 5438632, 1993.

[20] T. Jannson, "Real time Fourier transformation in dispersive optical fibers," Opt.Lett 8, 232, 1983.

[21] A. W. Lohmann and D. Mendlovic," Temporal filtering with time lenses," Applied Optics, 31, 6212-6219, 1992.

[22] D. Yang, S. Kumar and H. Wang, "Temporal filtering using time lenses for optical transmission systems", Opt. Commun., 2007, accepted for publication.

[23] J. Gowar, *Optical Communication System,* Prentice-Hall International Inc, 1984.

[24] G. P. Agrawal, *Fiber-Optic Communication Systems*, second edition, John Wiley & Sons Inc, 1997.

[25] D. Sadot and E. Boimovich, "Tunable optical filters for dense WDM networks", Communications Magazine, IEEE, 36, 50-55, 1998.

[26] R. Ghannam and W. Crossland, "Novel Wavelength-Tuneable Optical Filter for WDM Applications", Proc. of SPIE Vol. 6014, 2005.

[27] J. Stone and L. W. Stulz, "Pigtailed high finesse tunable FP interferometer with large, medium, and small FSR," Elect. Lett, 23, 781-83, 1987.